

# Selective Extraction of N<sub>2</sub> from Air by Diarylimine Iron Complexes

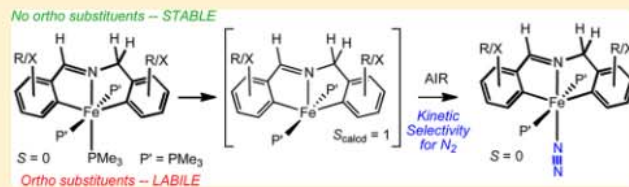
Erika R. Bartholomew,<sup>†</sup> Emily C. Volpe,<sup>†</sup> Peter T. Wolczanski,<sup>\*,†</sup> Emil B. Lobkovsky,<sup>†</sup> and Thomas R. Cundari<sup>‡</sup>

<sup>†</sup>Department of Chemistry & Chemical Biology, Baker Laboratory, Cornell University, Ithaca, New York 14853, United States

<sup>‡</sup>Department of Chemistry, Center for Advanced Scientific Computing and Modeling (CASCAM), University of North Texas, Box 305070, Denton, Texas 76203-5070, United States

## S Supporting Information

**ABSTRACT:** Treatment of *cis*-(Me<sub>3</sub>P)<sub>4</sub>FeMe<sub>2</sub> with *ortho*-substituted diarylimines afforded 2 equiv of MeH, PMe<sub>3</sub>, and {*mer-κC,N,C'*-(Ar-2-yl)CH<sub>2</sub>N-CH(Ar'-2-yl)}Fe(PMe<sub>3</sub>)<sub>3</sub> (Ar = 3,4,6-(F)<sub>3</sub>-C<sub>6</sub>H<sub>3</sub>, Ar' = 3,5-(CF<sub>3</sub>)<sub>2</sub>-C<sub>6</sub>H<sub>3</sub>, **1a**; Ar = 3,4,6-(F)<sub>3</sub>-C<sub>6</sub>H<sub>3</sub>, Ar' = 3,4,5-(F)<sub>3</sub>-C<sub>6</sub>H<sub>3</sub>, **1b**; Ar = 4,5,6-(F)<sub>3</sub>-C<sub>6</sub>H<sub>3</sub>, Ar' = 3,5-(CF<sub>3</sub>)<sub>2</sub>-C<sub>6</sub>H<sub>3</sub>, **1c**; Ar = C<sub>6</sub>H<sub>4</sub>, Ar' = 3-(OMe)-C<sub>6</sub>H<sub>3</sub>, **1d**; Ar = 4,5,6-(F)<sub>3</sub>-C<sub>6</sub>H<sub>3</sub>, Ar' = 3,6-Me<sub>2</sub>-C<sub>6</sub>H<sub>3</sub>, **1e**; Ar = C<sub>6</sub>H<sub>4</sub>, Ar' = 3,6-Me<sub>2</sub>-C<sub>6</sub>H<sub>3</sub>, **1f**). Exposure of **1a–f** to O<sub>2</sub> caused rapid degradation, but substitution of the unique PMe<sub>3</sub> with N<sub>2</sub> occurred when **1a–f** were exposed to air or N<sub>2</sub> (1 atm), yielding {*mer-κC,N,C'*-(Ar-2-yl)CH<sub>2</sub>N-CH(Ar'-2-yl)}Fe(PMe<sub>3</sub>)<sub>2</sub>L (L = N<sub>2</sub>, **2a–f**); CO, CNMe, and N<sub>2</sub>CPh<sub>2</sub> derivatives (L = CO, **3a–d,f**; L = CNMe, **8b**; L = N<sub>2</sub>CPh<sub>2</sub>, **9b**) were prepared. Dihydrogen or NH<sub>3</sub> binding to {*mer-κC,N,C'*-(3,4,6-(F)<sub>3</sub>-C<sub>6</sub>H<sub>2</sub>-2-yl)CH<sub>2</sub>N-CH(3,4,5-(F)<sub>3</sub>-C<sub>6</sub>H<sub>2</sub>-2-yl)}Fe(PMe<sub>3</sub>)<sub>2</sub> (**1b**, S = 1 (calc)) to provide **5b** (L = H<sub>2</sub>) or **6b** (L = NH<sub>3</sub>) was found comparable to that of N<sub>2</sub>, while PMe<sub>3</sub> (**1b**) and pyridine (L = py, **7b**) adducts were unfavorable. Protolytic conditions were modeled using HCCR as weak acids, and *trans*-{*κC,N*-(3,4,5-(F)<sub>3</sub>-C<sub>6</sub>H<sub>2</sub>)CH<sub>2</sub>N-CH(3,4,6-(F)<sub>3</sub>-C<sub>6</sub>H<sub>2</sub>-2-yl)}Fe(PMe<sub>3</sub>)<sub>3</sub>(CCR) (R = Me, **4b-Me**; R = Ph, **4b-Ph**) were generated from **1b**. Exposure of **1b** to N<sub>2</sub>O or N<sub>3</sub>SO<sub>2</sub>tol generated **2b** and Me<sub>3</sub>PO or Me<sub>3</sub>P-N(SO<sub>2</sub>)tol, respectively. Calculations revealed **2b** to be thermodynamically and kinetically favored over the *calculated* Fe(III) superoxide complex, <sup>3</sup>[FeO<sub>2</sub>], relative to **1b** + N<sub>2</sub> + O<sub>2</sub>. The correlation of **1b** + <sup>3</sup>O<sub>2</sub> to <sup>3</sup>[FeO<sub>2</sub>] is likely to have a relatively high intersystem crossing point (ICP) relative to **1b** + N<sub>2</sub> to **2b**, thereby explaining the dinitrogen selectivity.



## I. INTRODUCTION

The binding of dinitrogen to transition metals, most notably iron, is of historical and fundamental interest due to its activation and conversion to ammonia by nitrogenase enzymes<sup>1–13</sup> and in the heterogeneous iron- and ruthenium-catalyzed Haber–Bosch process (BASF, 1913).<sup>14–18</sup> The latter hydrogenation of dinitrogen to ammonia is arguably the most important industrial operation conducted on earth,<sup>14</sup> as it is the source of roughly  $5 \times 10^{11}$  kg of fertilizer as anhydrous ammonia, urea, ammonium nitrate (the nitrate is produced from oxidation of NH<sub>3</sub> via the Ostwald process), ammonium phosphates, and ammonium sulfate.<sup>18</sup> It has been estimated that >1% of the planet's energy supply is appropriated for Haber–Bosch operations and that >50% of the nitrogen in our body is derived from the fertilizer it generates.

Roughly 50 years after the Haber–Bosch process was initialized, evidence of the complexation of dinitrogen to Ru<sup>2+</sup> proved to be no less astonishing, as Allen and Seno's communication<sup>19</sup> was rejected for publication by *J. Am. Chem. Soc.* on the grounds that it was impossible.<sup>18</sup> Since the discovery and characterization of (H<sub>3</sub>N)<sub>3</sub>Ru(N<sub>2</sub>)<sup>2+</sup> salts,<sup>19–21</sup> a remarkable number of dinitrogen complexes have been synthesized,<sup>22–32</sup> and various bonding modes of N<sub>2</sub> have been realized,<sup>33–39</sup> some even leading to dinitrogen scission,<sup>40–48</sup> hydrogenation to ammonia,<sup>49–52</sup> catalytic reduc-

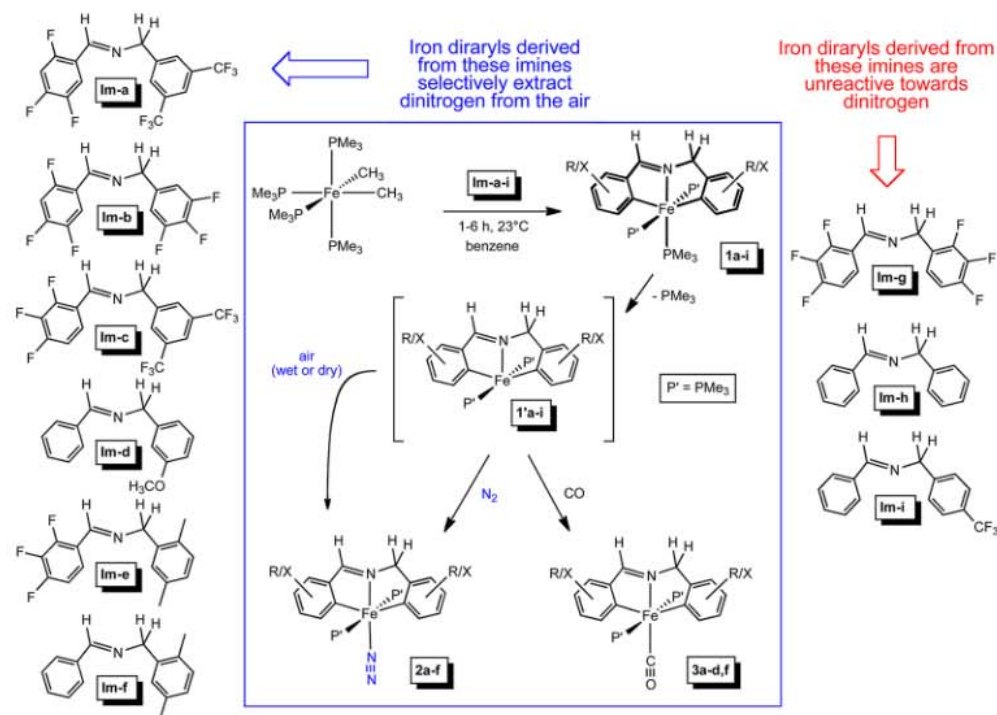
tions<sup>53–57</sup> that operate in cycles proposed by Chatt, Leigh, and Hidaï,<sup>22–28</sup> and related functionalizations.<sup>35–38,58–60</sup> The degree of dinitrogen activation, or the extent of reduction of N<sub>2</sub> upon binding, has often provided key examples of complexation and subsequent reduction.<sup>61,62</sup> As for modeling the Haber–Bosch process, the chemistry of nitrides,<sup>63–65</sup> in particular iron<sup>66–74</sup> and ruthenium nitrides,<sup>75,76</sup> and the conversion of this functionality to ammonia<sup>69,70,76</sup> has been a central focus.

Dinitrogen complexes of iron have been under intense scrutiny<sup>30–32,40,62,77–88</sup> due to the presence of iron in the nitrogenase cofactor responsible for the reduction of N<sub>2</sub> to two NH<sub>3</sub> and H<sub>2</sub> via 8 electrons and 8 protons (6 each for the N<sub>2</sub>; 2 each for the H<sub>2</sub>), which requires 16 equiv of Mg-ATP.<sup>1–13</sup> The majority of studies concerning iron-bound dinitrogen complexes utilize reducing equivalents provided by the metal or by exogenous agents and protons to effect the conversion to ammonia or hydrazine, i.e., Chatt, Leigh, etc. cycles.<sup>22–28</sup> Recently, dinitrogen reduction cycles utilizing iron have been developed in aqueous solution,<sup>83,84</sup> and model systems that feature two iron centers have been explored.<sup>86–88</sup>

Received: November 8, 2012

Published: January 30, 2013

Scheme 1



Somewhat lost in the excitement to ascertain the mechanism of biological dinitrogen reduction or new insights or improvements to the Haber–Bosch process are the fundamental aspects of selective dinitrogen binding, a factor critical in the processing of natural gas. Most specifications for natural gas require <4% N<sub>2</sub> in the feed stream, and dinitrogen removal processing techniques that rely on cryoscopic distillation, adsorption/desorption approaches, and even the latest membrane technologies are expensive.<sup>89–91</sup> In addition, methane can be a competitive binder in sieves and membranes, rendering these technologies more difficult to implement.

Dioxygen is normally an anathema to organometallic systems, and one would hardly expect to conduct dinitrogen binding reactions in its presence, unless an excess of exogenous reducing agent is employed. Consider the biological system pertaining to nitrogenase. In vivo, the NifEN protein delivers the FeMo-cofactor to its operational nitrogenase protein in a reducing environment,<sup>8–11</sup> while in vitro studies are typically done with dioxygen scrubbed from the system. However, there are some exceptions. Allen and Seno's (H<sub>3</sub>N)<sub>3</sub>RuN<sub>2</sub><sup>2+</sup> salt was shown to form in the presence of dioxygen,<sup>92</sup> and [HFe(dppe)<sub>2</sub>(THF)]<sup>+</sup> and H<sub>2</sub>(H<sub>2</sub>)Fe(PtPh<sub>2</sub>)<sub>4</sub> both form their respective dinitrogen complexes [HFe(dppe)<sub>2</sub>N<sub>2</sub>]<sup>+</sup><sup>93</sup> and H<sub>2</sub>(N<sub>2</sub>)Fe(PtPh<sub>2</sub>)<sub>4</sub><sup>94</sup> upon exposure to air.

Reported herein is the extraction of dinitrogen from the air by true iron organometallic complexes, which contain two iron–carbon bonds derived from diarylimine ligands that sterically and electronically tune the metal center for N<sub>2</sub> binding,<sup>95–97</sup> while rendering oxidative destruction by dioxygen kinetically unfavorable. Calculations on the system provide a rationale for the observed selectivity, and an assessment of how the compounds might be utilized for dinitrogen removal is provided.

## RESULTS

**Diarylimine Iron(II) Dinitrogen Complexes.** 1. *Discovery of N<sub>2</sub> Extraction from Air.* Diarylimine iron(III) complexes (i.e., [(mer-κC,N,C'-(Ar-2-yl)CH<sub>2</sub>N-CH(Ar-2-yl-X))Fe(PMe<sub>3</sub>)<sub>3</sub>OTf]) were previously examined as precursors to azaallyl ligands via deprotonation, but all attempts, even with bases such as LiN(TMS)<sub>2</sub>, regenerated the corresponding Fe(II) derivatives, {mer-κC,N,C'-(Ar-2-yl)CH<sub>2</sub>N-CH(Ar-2-yl-X)}Fe(PMe<sub>3</sub>)<sub>3</sub>. If deprotonation occurred, the resulting high-energy CNC<sup>nb</sup> orbital of the putative azaallyl complex {mer-κC,N,C'-(Ar-2-yl)CHNCH(Ar-2-yl-X)}Fe(PMe<sub>3</sub>)<sub>3</sub> was likely to internally transfer an electron to the Fe(III) center, generating an azaallyl radical that elicited hydrogen atom transfer to afford the Fe(II) product.<sup>98</sup>

One way of circumventing the internal oxidation would be to lower the CNC<sup>nb</sup> azaallyl orbital below the t<sub>2g</sub> set of the pseudo-octahedral Fe(III) species. As a consequence, fluorinated diarylimines were considered as a means to render the ligand more electron-withdrawing, and imine **Im-b** (Scheme 1) was readily synthesized via condensation of the inexpensive constituents 2,4,5-trifluorobenzaldehyde and 3,4,5-trifluorobenzylamine. Treatment of *cis*-(Me<sub>3</sub>P)<sub>4</sub>FeMe<sub>2</sub><sup>99</sup> with **Im-b** appeared to provide the diarylimine<sup>100–103</sup> tris-phosphine complex {mer-κC,N,C'-(3,4,5-(F)<sub>3</sub>-C<sub>6</sub>H-2-yl)CH<sub>2</sub>N-CH(3,4,6-(F)<sub>3</sub>-C<sub>6</sub>H-2-yl)}Fe(PMe<sub>3</sub>)<sub>3</sub> (**1b**), but upon examination after transfer to a dinitrogen-filled glovebox, only the dinitrogen complex *trans*-{mer-κC,N,C'-(3,4,5-(F)<sub>3</sub>-C<sub>6</sub>H-2-yl)CH<sub>2</sub>N-CH(3,4,6-(F)<sub>3</sub>-C<sub>6</sub>H-2-yl)}Fe(PMe<sub>3</sub>)<sub>2</sub>(N<sub>2</sub>) (**2b**) was observed. Moreover, the red color of **2b** persisted when the glassware used to prepare the complex was exposed to the air.

The apparent stability of the dinitrogen complex in the presence of air suggested that selective binding of dinitrogen was feasible; hence, *cis*-(Me<sub>3</sub>P)<sub>4</sub>FeMe<sub>2</sub> and **Im-b** were combined in a J. Young NMR tube into which benzene-*d*<sub>6</sub> was vacuum transferred. NMR spectroscopy confirmed the

Table 1. Dinitrogen and Carbonyl Stretching Frequencies for the Complexes  $\text{trans}\{\text{mer-}\kappa\text{C,N,C}'\text{-(Ar-2-yl)CH}_2\text{N-CH(Ar-2-yl)}\}\text{Fe}(\text{PMe}_3)_2\text{L}$  (L = N<sub>2</sub>, 2a–f; L = CO, 3a–d,f) and Stability  $t_{1/2}$  Values for 2a–f under Various Conditions (Wet Air, Atmospheric Conditions; Dry Air, Atmospheric Conditions with the Water Removed;  $p(\text{H}_2\text{O}) \approx 22\text{--}30$  Torr)

| Compound<br>P' = PMe <sub>3</sub> | L = NN<br>$\nu(\text{NN})$ (cm <sup>-1</sup> ) | L = CO<br>$\nu(\text{CO})$ (cm <sup>-1</sup> ) | L = NN<br>dry air (1 atm)<br>$t_{1/2}$ | L = NN<br>wet air (1 atm)<br>$t_{1/2}$ | L = NN<br>O <sub>2</sub> (1 atm)<br>$t_{1/2}$ |
|-----------------------------------|--|--|--|--|---|
|                                   | <b>2a</b> 2121                                 | <b>3a</b> 1950                                 | > 2 wks                                | 2 h                                    | < 10 min                                      |
|                                   | <b>2b</b> 2107                                 | <b>3b</b> 1936                                 | > 2 wks                                | 1.5 h                                  | < 20 min                                      |
|                                   | <b>2c</b> 2102                                 | <b>3c</b> 1921                                 | 2 h                                    | 1.3 h                                  | 30 min  |
|                                   | <b>2d</b> 2067                                 | <b>3d</b> 1896                                 | > 1 wk                                 | 2 h                                    | 30 min  |
|                                   | <b>2e</b> 2058                                 |  | 2 h                                    | 1 h                                    | < 10 min                                      |
|                                   | <b>2f</b> 2046                                 | <b>3f</b> 1882                                 | > 2 wks                                | 2 h                                    | 30 min  |

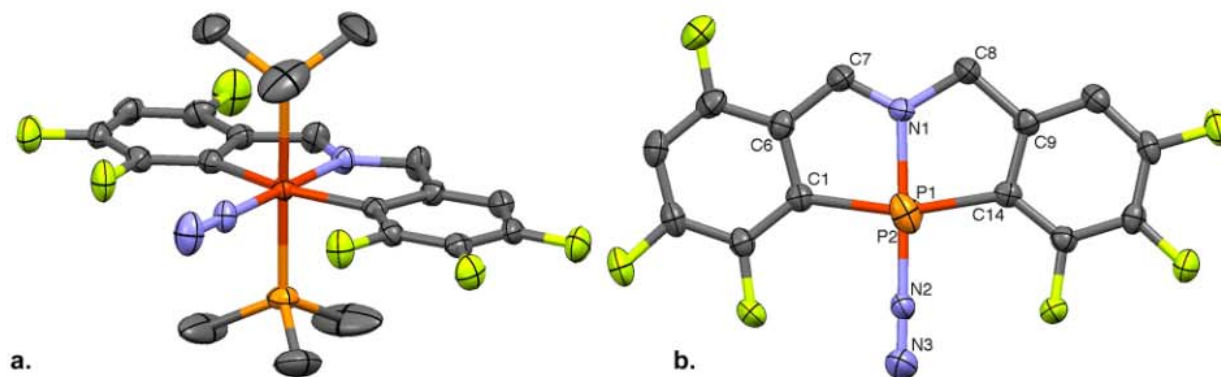
preparation of **1b** after 1–6 h. Air was admitted to the tube, and it was vigorously shaken; a second NMR spectrum indicated a mixture of **1b** and **2b**, and further admissions of air afforded a complete conversion to the dinitrogen complex **2b**.

**2. Scope of Dinitrogen Complexes.** Inductively, the electron-withdrawing fluorines on **Im-b** should attenuate  $\pi$ -back-bonding to N<sub>2</sub>. In contradiction of this logic, the six fluorine substituents were initially considered as an electronic feature that somehow elicited selective dinitrogen extraction over dioxygen from air. Those considerations were rapidly dashed as *cis*-(Me<sub>3</sub>P)<sub>4</sub>FeMe<sub>2</sub> was treated with (2,3,4-(F)<sub>3</sub>-C<sub>6</sub>H<sub>2</sub>)CH<sub>2</sub>N-CH(2,3,4-(F)<sub>3</sub>-C<sub>6</sub>H<sub>2</sub>) (**Im-g**), a diarylimine considered to have an electron-withdrawing capacity similar to that of **Im-b**, but without ortho substituents. Formation of the triphosphine complex {*mer-kappa-C,N,C'*-(4,5,6-(F)<sub>3</sub>-C<sub>6</sub>H<sub>2</sub>-2-yl)CH<sub>2</sub>N-CH(4,5,6-(F)<sub>3</sub>-C<sub>6</sub>H<sub>2</sub>-2-yl)}Fe(PMe<sub>3</sub>)<sub>3</sub> (**1g**) was noted, but the complex did not react with dinitrogen. Clearly the electron-withdrawing capacity of the diarylimine did not appear to matter significantly. The result corroborated previous findings that {*mer-kappa-C,N,C'*-(C<sub>6</sub>H<sub>4</sub>-2-yl)CH<sub>2</sub>N-CH(C<sub>6</sub>H<sub>4</sub>-2-yl)}Fe(PMe<sub>3</sub>)<sub>3</sub> (**1h**) and {*mer-kappa-C,N,C'*-(5-(CF<sub>3</sub>)-C<sub>6</sub>H<sub>2</sub>-2-yl)CH<sub>2</sub>N-CH(C<sub>6</sub>H<sub>4</sub>-2-yl)}Fe(PMe<sub>3</sub>)<sub>3</sub> (**1i**) were also impervious to substitution by dinitrogen.

Another previously explored derivative, {*mer-kappa-C,N,C'*-(6-(OCH<sub>3</sub>)-C<sub>6</sub>H<sub>4</sub>-2-yl)CH<sub>2</sub>N-CH(C<sub>6</sub>H<sub>4</sub>-2-yl)}Fe(PMe<sub>3</sub>)<sub>3</sub> (**1d**),<sup>98</sup> whose methoxy-substituted diarylimine ligand was considered to be significantly more electron donating than **Im-b**, had only been prepared on an NMR tube scale and had not been exposed to N<sub>2</sub>. An attempted isolation of **1d** under a nitrogen atmosphere instead yielded the dinitrogen derivative

*trans*-{*mer-kappa-C,N,C'*-(6-(OCH<sub>3</sub>)-C<sub>6</sub>H<sub>4</sub>-2-yl)CH<sub>2</sub>N-CH(C<sub>6</sub>H<sub>4</sub>-2-yl)}Fe(PMe<sub>3</sub>)<sub>2</sub>(N<sub>2</sub>) (**2d**) in 80% yield. Scheme 1 shows that a group of diarylimines, ranging from the most electron withdrawing (3,5-(CF<sub>3</sub>)<sub>2</sub>-C<sub>6</sub>H<sub>3</sub>)CH<sub>2</sub>N-CH(2,4,5-(F)<sub>3</sub>-C<sub>6</sub>H<sub>2</sub>) (**Im-a**) to the modestly electron donating (2,5-Me<sub>2</sub>-C<sub>6</sub>H<sub>3</sub>)-CH<sub>2</sub>N-CH(C<sub>6</sub>H<sub>5</sub>) (**Im-f**), afforded the dinitrogen complexes *trans*-{*mer-kappa-C,N,C'*-(Ar-2-yl)CH<sub>2</sub>N-CH(Ar-2-yl)}Fe(PMe<sub>3</sub>)<sub>2</sub>(N<sub>2</sub>) (**2a–f**). All of the dinitrogen complexes selectively extract N<sub>2</sub> from air, and they all have substituents ortho to the activated aryl positions; only one ortho substituent appears necessary to cause PMe<sub>3</sub> substitution. IR spectra of **2a–f** revealed the expected inverse correlation of dinitrogen stretching frequencies vs electron-withdrawing capacity of each diarylimine (Table 1). The order suggests that ortho substituents are more important and that the inductive influence of the *o*-methoxy group of **2d** outweighs its  $\pi$ -donor capacity.

**3. Diarylimine Tris-PMe<sub>3</sub> Iron Intermediates.** In order to observe the putative tris-PMe<sub>3</sub> precursors to the dinitrogen complexes, *cis*-(Me<sub>3</sub>P)<sub>4</sub>FeMe<sub>2</sub> was treated with **Im-a–Im-f** in NMR tube scale reactions where dinitrogen was kept from the system. NMR spectra corresponding to diamagnetic {*mer-kappa-C,N,C'*-(Ar-2-yl)CH<sub>2</sub>N-CH(Ar-2-yl)}Fe(PMe<sub>3</sub>)<sub>3</sub> were obtained for **1b,d**, whereas chemical shifts and line widths consistent with paramagnetic complexes were observed for **1a,c,e,f**. Evans method<sup>104</sup> studies on the crude solutions of **1a,c,e,f** afforded  $\mu_{\text{eff}}$  values ranging from 3.0 to 3.3  $\mu_{\text{B}}$ , which are consistent with plausible *S* = 1 ground states possessing significant contributions from spin–orbit coupling.<sup>105</sup> The spectra for **1b,d** were similar to that of **1g** and those previously



**Figure 1.** (a) Molecular view (50% probability ellipsoids) of *trans*-{*mer*- $\kappa$ C,N,C'-(3,4,5-(F)<sub>3</sub>-C<sub>6</sub>H-2-yl)CH<sub>2</sub>N-CH(3,4,6-(F)<sub>3</sub>-C<sub>6</sub>H-2-yl)}Fe(PMe<sub>3</sub>)<sub>2</sub>(N<sub>2</sub>) (**2b**) and (b) a view down the P–Fe–P axis with the phosphine methyl groups removed. Selected bond distances (Å) and angles (deg): Fe–C1, 1.996(2); Fe–C14, 2.014(2); Fe–N1, 1.935(2); Fe–N2, 1.811(2); Fe–P1, 2.2292(7); Fe–P2, 2.2389(7); N2–N3, 1.104(3); N1–C7, 1.308(3); N1–C8, 1.459(3); C6–C7, 1.443(3); C8–C9, 1.501(4); N1–Fe–N2, 178.17(10); C1–Fe–C14, 163.06(9); P1–Fe–P2, 176.04(3); N1–Fe–C1, 81.25(9); N1–Fe–C14, 81.82(9); N1–Fe–P1, 91.47(6); N1–Fe–P2, 91.32(6); N2–Fe–P1, 89.54(7); N2–Fe–P2, 87.74(7); C1–Fe–P1, 91.62(7); C14–Fe–P1, 89.13(7); C1–Fe–P2, 91.59(7); C14–Fe–P2, 88.49(6); C1–Fe–N2, 97.20(9); C14–Fe–N2, 99.73(9); Fe–N2–N3, 178.9(2); Fe–C1–C2, 134.17(19); Fe–C1–C6, 111.81(15); Fe–C14–C13, 131.84(16); Fe–C14–C9, 113.79(18).

recorded for **1h,i**, including the diagnostic A<sub>2</sub>B pattern in the <sup>31</sup>P{<sup>1</sup>H} NMR that was used to verify the meridional conformation, including *J*<sub>PP</sub> values of 58 (**1b**), 62 (**1d**), and 61 Hz (**1g**).<sup>98</sup>

It is plausible that significant dissociation of PMe<sub>3</sub> to the *ve*-coordinate {*mer*- $\kappa$ C,N,C'-(Ar-2-yl)CH<sub>2</sub>N-CH(Ar-2-yl)}Fe(PMe<sub>3</sub>)<sub>2</sub> (**1 a,c,e,f**) complexes, which are likely to be triplets according to DFT calculations, occurs for these complexes. The spectrum of *trans*-{*mer*- $\kappa$ C,N,C'-(3,5-(CF<sub>3</sub>)<sub>2</sub>-C<sub>6</sub>H<sub>3</sub>)CH<sub>2</sub>N-CH(2,4,5-(F)<sub>3</sub>-C<sub>6</sub>H<sub>2</sub>)}Fe(PMe<sub>3</sub>)<sub>3</sub> (**1a**) contradicts this possibility, as paramagnetically shifted <sup>1</sup>H NMR spectral resonances for the unique phosphine ( $\delta$  –11.46) and *trans*-PMe<sub>3</sub> ( $\delta$  –4.86) groups are observed in addition to that of free PMe<sub>3</sub>. Rapid exchange with free PMe<sub>3</sub> via a dissociative process is thereby ruled out, and it appears unlikely that *ve*-coordinate **1 a** impacts the spectrum of **1a**.

The <sup>1</sup>H NMR spectra of **1c,e,f** are broader and fewer features are revealed, including overlapping resonances for the distinct PMe<sub>3</sub> sites. The <sup>1</sup>H NMR spectrum of **1c** included a resonance for free PMe<sub>3</sub>; thus, it is likely that its unique PMe<sub>3</sub> is bound strongly enough not to exchange with the free ligand on the time scale of the NMR observation. DFT calculations indicated that *S* = 0 and *S* = 1 states were close in energy for the trisphosphine complexes (vide infra).

**4. Structure of *trans*-{*mer*- $\kappa$ C,N,C'-(3,4,5-(F)<sub>3</sub>-C<sub>6</sub>H-2-yl)CH<sub>2</sub>N-CH(3,4,6-(F)<sub>3</sub>-C<sub>6</sub>H-2-yl)}Fe(PMe<sub>3</sub>)<sub>2</sub>(N<sub>2</sub>) (**2b**).** The molecular structure of *trans*-{*mer*- $\kappa$ C,N,C'-(3,4,5-(F)<sub>3</sub>-C<sub>6</sub>H-2-yl)CH<sub>2</sub>N-CH(3,4,6-(F)<sub>3</sub>-C<sub>6</sub>H-2-yl)}Fe(PMe<sub>3</sub>)<sub>2</sub>(N<sub>2</sub>) (**2b**) was determined by single-crystal X-ray diffraction techniques, and views of the complex are given in Figure 1. A limited amount of crystallographic and refinement data are given in Table 2. A relatively short *d*(N–N)<sup>30</sup> value of 1.104(3) Å is observed in concert with the  $\nu$ (NN) of 2107 cm<sup>–1</sup> observed in its IR spectrum, and the *d*(Fe–NN) value of 1.811(2) is significantly shorter than the iron–imine distance of 1.935(2) Å, but both are within normal ranges. The iron–aryl bond distances are 1.996(2) and 2.014(2) Å, which are again short but are in range of those for other arene-activated species derived from (Me<sub>3</sub>P)<sub>4</sub>FeMe<sub>2</sub>.<sup>100–103</sup> The most significant metric parameter is the C1–Fe–C14 bite angle of 163.06(9)° and its complementary C1–Fe–N2 and C14–Fe–N2 angles of 97.20(9) and

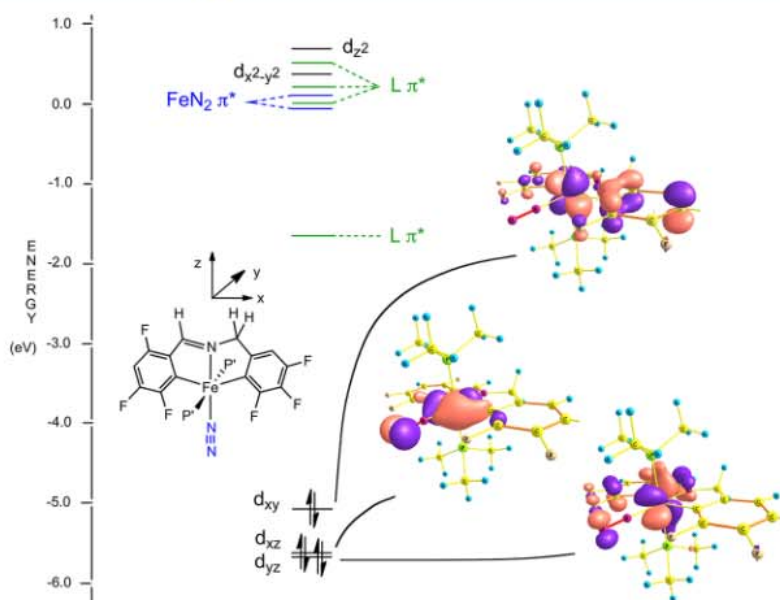
**Table 2. Selected Crystallographic and Refinement Data for *trans*-{*mer*- $\kappa$ C,N,C'-(3,4,5-(F)<sub>3</sub>-C<sub>6</sub>H-2-yl)CH<sub>2</sub>N-CH(3,4,6-(F)<sub>3</sub>-C<sub>6</sub>H-2-yl)}Fe(PMe<sub>3</sub>)<sub>2</sub>(N<sub>2</sub>) (**2b**) and *trans*-{*mer*- $\kappa$ C,N,C'-(3,4,5-(F)<sub>3</sub>-C<sub>6</sub>H-2-yl)CH<sub>2</sub>N-CH(3,4,6-(F)<sub>3</sub>-C<sub>6</sub>H-2-yl)}Fe(PMe<sub>3</sub>)<sub>2</sub>Cl (**12b**).**

|  | <b>2b</b>   | <b>12b</b>  |
|--|---|---|
| formula  | C <sub>20</sub> H <sub>23</sub> F <sub>6</sub> N <sub>3</sub> P <sub>2</sub> Fe | C <sub>20</sub> H <sub>23</sub> F <sub>6</sub> NP <sub>2</sub> ClFe |
| formula wt   | 537.20  | 544.63  |
| space group  | Cc  | P2 <sub>1</sub> /c  |
| Z  | 4   | 4   |
| <i>a</i> , Å   | 19.0597(7)  | 10.6916(9)  |
| <i>b</i> , Å   | 9.1733(4)   | 8.1275(7)   |
| <i>c</i> , Å   | 15.7972(10)   | 26.737(2)   |
| $\alpha$ , deg   | 90  | 90  |
| $\beta$ , deg  | 121.8450(10)  | 100.653(4)  |
| $\gamma$ , deg   | 90  | 90  |
| <i>V</i> , Å <sup>3</sup>                                      | 2346.2(2)   | 2283.3(3)   |
| $\rho_{\text{calc}}$ , g cm <sup>–3</sup>                      | 1.521   | 1.584   |
| $\mu$ , mm <sup>–1</sup>                                       | 0.839   | 0.974   |
| temp, K  | 173(2)  | 173(2)  |
| $\lambda$ (Å)  | 0.71073   | 0.71073   |
| R indices ( <i>I</i> > 2 $\sigma$ ( <i>I</i> )) <sup>a,b</sup> | R1 = 0.0364<br>wR2 = 0.0815   | R1 = 0.0370<br>wR2 = 0.0903   |
| R indices (all data) <sup>a,b</sup>                            | R1 = 0.0434<br>wR2 = 0.0858   | R1 = 0.0528<br>wR2 = 0.1004   |
| GOF <sup>c</sup>   | 1.024   | 1.023   |

<sup>a</sup>R1 =  $\sum ||F_o| - |F_c|| / \sum |F_o|$ . <sup>b</sup>wR2 =  $[\sum w(|F_o| - |F_c|)^2 / \sum wF_o^2]^{1/2}$ . <sup>c</sup>GOF (all data) =  $[\sum w(|F_o| - |F_c|)^2 / (n - p)]^{1/2}$ ; *n* = number of independent reflections, *p* = number of parameters.

99.73(9)°, respectively. The bite angle of the diarylimine is critical, because it is consequential to  $\sigma^*/d_{xz}$  mixing within the diarylimine plane that permits greater overlap and a better energy match with the N( $\pi^*$ ) orbital, thereby enhancing back-bonding. The remaining core angles among adjacent sites average 90.1(16)°, and the N1–Fe–N2 and P1–Fe–P2 angles are 178.17(10) and 176.04(3)°, respectively.

**5. Molecular Orbital View of  $\pi$ -Back-Bonding to N<sub>2</sub>.** Figure 2 illustrates a truncated molecular orbital diagram of *trans*-{*mer*- $\kappa$ C,N,C'-(3,4,5-(F)<sub>3</sub>-C<sub>6</sub>H-2-yl)CH<sub>2</sub>N-CH(3,4,6-(F)<sub>3</sub>-C<sub>6</sub>H-2-yl)}Fe(PMe<sub>3</sub>)<sub>2</sub>(N<sub>2</sub>) (**2b**), highlighting the *t*<sub>2g</sub>,  $\pi$ -back-



**Figure 2.** Truncated molecular orbital diagram of *trans*-{*mer*- $\kappa$ C,N,C'-(3,4,5-(F)<sub>3</sub>-C<sub>6</sub>H-2-yl)CH<sub>2</sub>N-CH(3,4,6-(F)<sub>3</sub>-C<sub>6</sub>H-2-yl)}Fe(PMe<sub>3</sub>)<sub>2</sub>(N<sub>2</sub>) (**2b**) showing the greater  $\pi$  back-bonding from the  $d_{xz}$  orbital relative to  $d_{yz}$  as a consequence of  $\sigma^*/d_{xz}$  mixing.

bonding set of orbitals. Despite the electron-withdrawing capability of the hexa fluorinated diarylimine ligand, efficient back-bonding to dinitrogen occurs because of the aforementioned mixing of diaryl to  $\sigma^*$  character with  $d_{xz}$ , rendering the orbital better at back-bonding. If the bite angle is assumed to be similar for the remaining imines, the stability of all the dinitrogen complexes is well justified. Note that the diagram also reveals a low-lying diarylimine  $\pi^*$  orbital. It is likely that most of the color variations of the dinitrogen and related complexes stem from MLCT bands in the visible region that are derived from occupation of this orbital. The  $\sigma^*$  orbitals  $d_{x^2-y^2}$  and  $d_{z^2}$  are buried amidst a number of diarylimine and iron–dinitrogen  $\pi^*$  orbitals. The energies are given in eV, but the values of virtual vs filled orbitals are likely to be inaccurate, although relatively accurate within each set.<sup>106–108</sup>

#### 6. Stability of Dinitrogen Complexes in Air and Dioxygen.

Table 1 gives degradation  $t_{1/2}$  values for the disappearance of dinitrogen complexes **2a–f** under normal air (wet), dry air, and pure dioxygen conditions, all at 1 atm. The experiments were conducted in J. Young NMR tubes, which were exposed to the particular atmospheric conditions, vigorously shaken, monitored by <sup>1</sup>H NMR spectroscopy, and periodically refreshed. The longest-lived samples had  $t_{1/2}$  values of over 2 weeks in dry air, although a few samples persisted for only a few hours. In normal wet air, samples had much shorter degradation  $t_{1/2}$  values of 1–2 h, suggesting that the most rapid decomposition mode involved protonation. Free diarylimine was typically observed to grow in as the presumed protolytic degradation proceeded. In samples of pure O<sub>2</sub> (1 atm), the  $t_{1/2}$  values were the shortest, ranging from <10 to 30 min. Virtually no correlation with substituents was noted, as among the most long-lived were both electron-withdrawing and electron-donating diarylimine chelates. As a consequence, it does not appear that outer-sphere electron transfer (eT) to dioxygen is a particularly credible degradation path.

Dioxygen (1.0 atm) degradation  $t_{1/2}$  values were in most cases substantially shorter than those in dry air (~0.2 atm of O<sub>2</sub>). For example, the <20 min vs >2 weeks for **2b** corresponds

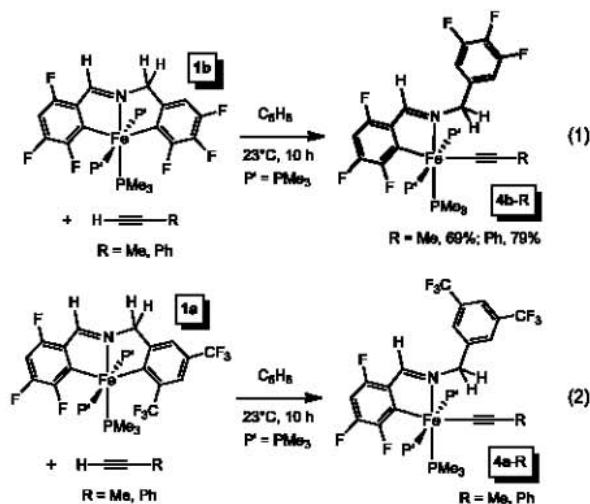
to a >1000 rate of degradation difference (a rough first-order decay was observed) that cannot be simply accounted for by the approximate factor of 5 difference in [O<sub>2</sub>] in solution and above. Only for **2c** was the degradation rate as fast in dry air as it was in 1 atm of O<sub>2</sub> once the difference in [O<sub>2</sub>] was taken account. Assuming dinitrogen dissociation is the initial step, these experiments suggest there is a kinetic preference for dinitrogen binding; otherwise, the dry air and 1 atm dioxygen conditions would yield degradation  $t_{1/2}$  values that are near a factor of 4. The selective, reversible binding of N<sub>2</sub> in dry air is a plausible explanation for the difference vs the fast degradation in 1 atm of O<sub>2</sub>. The dinitrogen ligand, at least on **2b**-<sup>15</sup>N<sub>2</sub>, cannot be rapidly and reversibly lost, nor does N <sub>$\alpha$</sub>  ( $\delta$  369.55 relative to NH<sub>3</sub>(l)) rapidly interconvert with N <sub>$\beta$</sub>  ( $\delta$  334.15), since a <sup>1</sup>J<sub>N<sub>1</sub>N<sub>2</sub> value of 4 Hz is resolved in the <sup>15</sup>N NMR spectrum.<sup>109</sup></sub>

It is tempting to conclude that the  $t_{1/2}$  values in 1 atm of dioxygen reflect the rates of irreversible dinitrogen loss. Without independent studies, associative or associative interchange paths cannot be dismissed under these pseudo-first-order conditions. A purely dissociative path might correlate with the  $\nu$ (NN) of **2a–f**, as the lower stretching frequencies could be construed as indicative of stronger binding; no such correlation is evident, given that **2e** (2058 cm<sup>-1</sup>) is one of the swiftest to degrade under 1 atm of O<sub>2</sub> and **2c** (2102 cm<sup>-1</sup>) is one of the slowest. It is interesting to note that {*mer*- $\kappa$ C,N,C'-(4,5,6-(F)<sub>3</sub>-C<sub>6</sub>H-2-yl)CH<sub>2</sub>N-CH(4,5,6-(F)<sub>3</sub>-C<sub>6</sub>H-2-yl)}Fe(PMe<sub>3</sub>)<sub>3</sub> (**1g**), a tris-PMe<sub>3</sub> derivative with no ortho substituents, was stable to 1 atm of O<sub>2</sub> for >2 weeks.

The degradation path in 1 atm of O<sub>2</sub>, aside from the disappearance of **2a–f**, is not obvious. No organic materials are observed in the <sup>1</sup>H NMR spectra of the orange solutions other than **2a–f**, and Evans method<sup>104</sup> measurements on samples monitored to greater than 95% completion afford  $\mu_{eff}$  values ranging from 3.1 to 3.5  $\mu_B$ . While 1 atm of O<sub>2</sub> is known to broaden signals, it typically does not make them disappear. The possibility of paramagnetic {*mer*- $\kappa$ C,N,C'-(Ar-2-yl)CH<sub>2</sub>N-CH(Ar-2-yl)}Fe(PMe<sub>3</sub>)<sub>2</sub>(O<sub>2</sub>) complexes was considered in

view of calculations indicative of an Fe(III) superoxide possessing a triplet GS. IR studies failed to elicit bands in the regions expected, and crystalline material obtained from the J. Young tubes was identified as  $\text{Me}_3\text{PO}$ , consistent with oxidative destruction. An NMR silent  $\text{C}_6\text{D}_6$  solution of **2b** was subjected to an aqueous quench, and  $^1\text{H}$  NMR spectral analysis of this mixture revealed **Im-b** and  $\text{Me}_3\text{PO}$  along with a solid. It is conceivable that the  $\text{O}_2$  degradations generate paramagnetic  $\text{L}_n\text{FeO}_x$  aggregates that have a significant effect on the observation of NMR spectra. In support of this proposal, treatment of  $\{\text{mer-}\kappa\text{C},\text{N},\text{C}'\text{-}(3,4,5\text{-}(\text{F})_3\text{-C}_6\text{H}_2\text{-yl})\text{CH}_2\text{N-CH}(3,4,6\text{-}(\text{F})_3\text{-C}_6\text{H}_2\text{-yl})\}\text{Fe}(\text{PMe}_3)_3$  (**1b**) with 1 atm of  $\text{O}_2$  generated a black solid, but no observable  $\text{Me}_3\text{PO}$  or free **Im-b** was observed by NMR spectroscopy.

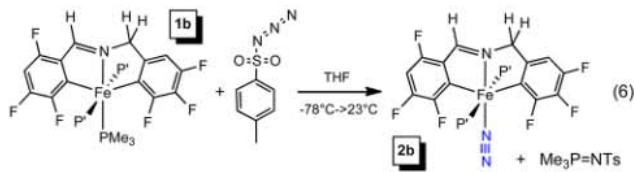
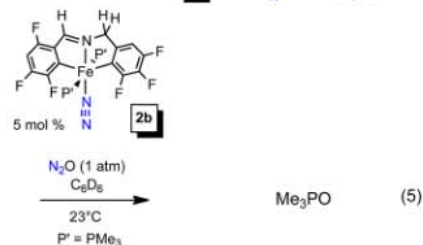
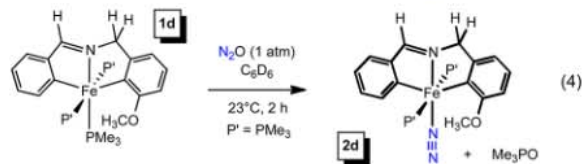
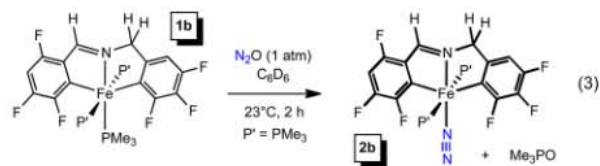
**7. Terminal Alkynes as Proton Donors.** Attempts to view hydrolysis intermediates via the addition of 1 equiv of  $\text{H}_2\text{O}$  to  $\text{trans-}\{\text{mer-}\kappa\text{C},\text{N},\text{C}'\text{-}(3,4,5\text{-}(\text{F})_3\text{-C}_6\text{H}_2\text{-yl})\text{CH}_2\text{N-CH}(3,4,6\text{-}(\text{F})_3\text{-C}_6\text{H}_2\text{-yl})\}\text{Fe}(\text{PMe}_3)_3$  (**1b**) invariably led to complete degradation of a portion of the starting dinitrogen complex; hence, terminal alkynes were considered as weakly acidic substrates that would allow observation of intermediates derived from proton transfer. Treatment of **1b** with HCCR ( $\text{R} = \text{Me}, \text{Ph}$ ) afforded  $\text{trans-}\{\kappa\text{C},\text{N}\text{-}(3,4,5\text{-}(\text{F})_3\text{-C}_6\text{H}_2\text{-yl})\text{CH}_2\text{N-CH}(3,4,6\text{-}(\text{F})_3\text{-C}_6\text{H}_2\text{-yl})\}\text{Fe}(\text{PMe}_3)_3(\text{CCR})$  ( $\text{R} = \text{Me}, \mathbf{4b}\text{-Me}$ , 69%,  $\nu(\text{CC})$  2081  $\text{cm}^{-1}$ ;  $\text{R} = \text{Ph}, \mathbf{4b}\text{-Ph}$ , 79%,  $\nu(\text{CC})$  2050  $\text{cm}^{-1}$ ) as dark red solids. As eq 1 indicates, protonation of



the  $(3,4,5\text{-}(\text{F})_3\text{-C}_6\text{H}_2\text{-yl})\text{CH}_2\text{-}$  group has occurred to generate a dangling benzyl group attached to the  $\kappa\text{C},\text{N}$ -phenylimine residue. The three phosphines remain in a meridional conformation, while the acetylides are likely to occupy the sterically hindered site opposite the aryl and between the imine and unique  $\text{PMe}_3$ , although the NMR spectra do not distinguish this structure from one in which the acetylide and  $\text{PMe}_3$  positions are reversed. Note that the slightly longer Fe–Ar bond (2.014(2) Å relative to 1.996(2) Å) has been protonated, but whether this is a kinetic or thermodynamic product was not ascertained. Exposure to excess HCCR removed the diarylimine entirely and afforded  $\text{trans-}(\text{Me}_3\text{P})_4\text{Fe}(\text{CCR})_2$  as one of the products. Protonation of the Fe–Ar bond on the benzylic side of the diarylimine seems general, as  $\text{trans-}\{\text{mer-}\kappa\text{C},\text{N},\text{C}'\text{-}(3,5\text{-}(\text{CF}_3)_2\text{-C}_6\text{H}_2\text{-yl})\text{CH}_2\text{N-CH}(3,4,6\text{-}(\text{F})_3\text{-C}_6\text{H}_2\text{-yl})\}\text{Fe}(\text{PMe}_3)_3$  (**1a**) was also converted to  $\text{trans-}\{\kappa\text{C},\text{N}\text{-}(3,5\text{-}(\text{CF}_3)_2\text{-C}_6\text{H}_3)\text{CH}_2\text{N-CH}(3,4,6\text{-}(\text{F})_3\text{-C}_6\text{H}_2\text{-yl})\}\text{Fe}(\text{PMe}_3)_3(\text{CCR})$  ( $\text{R} = \text{Me}, \mathbf{4a}\text{-Me}$ ,  $\nu(\text{CC})$  2077  $\text{cm}^{-1}$ ;  $\text{R} = \text{Ph}$ ,

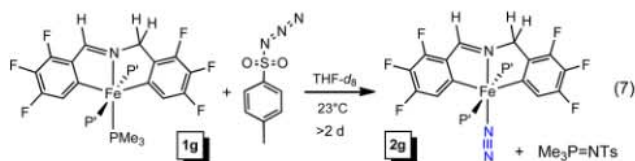
**4a-Ph**,  $\nu(\text{CC})$  2044  $\text{cm}^{-1}$ , eq 2) by HCCR; no attempts at isolation were made.

**8. Alternate Route to  $\text{N}_2$  Complexes via  $\text{N}_2\text{O}$ .** While exploring the synthesis of diarylimine diphosphine Fe(II) adducts,  $\{\text{mer-}\kappa\text{C},\text{N},\text{C}'\text{-}(3,4,5\text{-}(\text{F})_3\text{-C}_6\text{H}_2\text{-yl})\text{CH}_2\text{N-CH}(3,4,6\text{-}(\text{F})_3\text{-C}_6\text{H}_2\text{-yl})\}\text{Fe}(\text{PMe}_3)_3$  (**1b**) and  $\text{trans-}\{\text{mer-}\kappa\text{C},\text{N},\text{C}'\text{-}(3\text{-OMe})\text{-C}_6\text{H}_3\text{-2-yl})\text{CH}_2\text{N-CH}(\text{C}_6\text{H}_4\text{-2-yl})\}\text{Fe}(\text{PMe}_3)_3$  (**1d**) were treated with  $\text{N}_2\text{O}^{110}$  on NMR tube scales, but the corresponding dinitrogen derivatives  $\text{trans-}\{\text{mer-}\kappa\text{C},\text{N},\text{C}'\text{-}(3,4,5\text{-}(\text{F})_3\text{-C}_6\text{H}_2\text{-yl})\text{CH}_2\text{N-CH}(3,4,6\text{-}(\text{F})_3\text{-C}_6\text{H}_2\text{-yl})\}\text{Fe}(\text{PMe}_3)_2(\text{N}_2)$  (**2b**) and  $\text{trans-}\{\text{mer-}\kappa\text{C},\text{N},\text{C}'\text{-}(3\text{-OMe})\text{-C}_6\text{H}_3\text{-2-yl})\text{CH}_2\text{N-CH}(\text{C}_6\text{H}_4\text{-2-yl})\}\text{Fe}(\text{PMe}_3)_2(\text{N}_2)$  (**2d**), respectively, were formed instead according to eqs 3 and 4



(>95%). Compound **2b** was subsequently found to be a very modest catalyst for the conversion of  $\text{PMe}_3$  to  $\text{Me}_3\text{PO}$  with  $\text{N}_2\text{O}$  with a pseudo-first-order rate constant of  $\sim 4 \times 10^{-4} \text{ s}^{-1}$  at 23 °C (eq 5). This is roughly a factor of 500 faster than the uncatalyzed rate constant of  $\sim 8 \times 10^{-7} \text{ s}^{-1}$  under identical conditions.

Since **2b** failed to catalyze oxygen atom transfer from  $\text{N}_2\text{O}$  to any useful substrates (i.e., olefins etc.), the reactivity was not examined further. A related nitrene transfer<sup>64,111,112</sup> from tosyl azide to  $\text{PMe}_3$  was noted (eq 6), and the reaction proved to be somewhat sporadic, but useful. The alternative nitrous oxide method failed to generate the dinitrogen complex from  $\text{trans-}\{\text{mer-}\kappa\text{C},\text{N},\text{C}'\text{-}(4,5,6\text{-}(\text{F})_3\text{-C}_6\text{H}_2\text{-yl})\text{CH}_2\text{N-CH}(4,5,6\text{-}(\text{F})_3\text{-C}_6\text{H}_2\text{-yl})\}\text{Fe}(\text{PMe}_3)_3$  (**1g**), but the nitrene transfer reagent cleanly effected the transformation on an NMR tube scale (eq 7). The generation of  $\text{trans-}\{\text{mer-}\kappa\text{C},\text{N},\text{C}'\text{-}(4,5,6\text{-}(\text{F})_3\text{-C}_6\text{H}_2\text{-yl})\text{CH}_2\text{N-CH}(4,5,6\text{-}(\text{F})_3\text{-C}_6\text{H}_2\text{-yl})\}\text{Fe}(\text{PMe}_3)_2(\text{N}_2)$  (**2g**) permitted measurement of its  $\nu(\text{NN})$  value of 2070  $\text{cm}^{-1}$ , which revealed that having two *o*-F substituents (cf. **2b**, 2107  $\text{cm}^{-1}$ ) rather than one meta and one para renders the diarylimine of **2b** substantially more inductively withdrawing.



**Related Diarylimine Fe(II) Adducts. 1. Carbonyl Derivatives.** As shown in Scheme 1, a select number of related carbonyl derivatives were generated, some via isolation and others on NMR tube scales, as a check on how the substituents affected the  $\nu(\text{CO})$  values in the infrared spectra. Table 1 indicates that the  $\nu(\text{CO})$  of  $\{\text{mer-}\kappa\text{C},\text{N},\text{C}'\text{-}(\text{Ar-2-yl})\text{CH}_2\text{N-CH}(\text{Ar-2-yl})\}\text{Fe}(\text{PMe}_3)_2(\text{CO})$  (**3a–d,f**) reveal a trend identical with that of the dinitrogen derivatives, with roughly the same spread in values. The values range from 1950 to 1882  $\text{cm}^{-1}$ , which are fairly low for Fe(II) species, and provide another indication of the unique back-bonding situation illustrated in Figure 2.

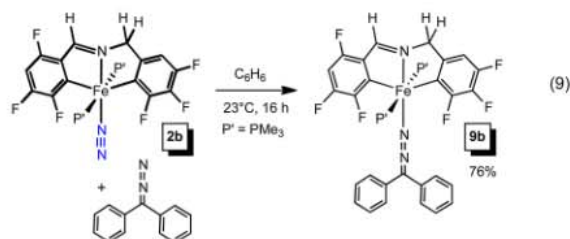
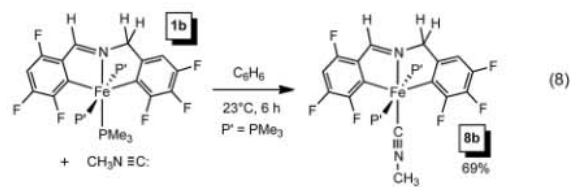
**2.  $\text{NH}_3$ ,  $\text{PMe}_3$ , and  $\text{H}_2$  Binding Studies.** Scheme 2 shows rough equilibrium constants ( $K_c$ ; all components relative to 1 M) measured for the formation of  $\text{trans-}\{\text{mer-}\kappa\text{C},\text{N},\text{C}'\text{-}(3,4,5\text{-}(\text{F})_3\text{-C}_6\text{H-2-yl})\text{CH}_2\text{N-CH}(3,4,6\text{-}(\text{F})_3\text{-C}_6\text{H-2-yl})\}\text{Fe}(\text{PMe}_3)_2(\text{N}_2)$  (**2b**) from  $\text{trans-}\{\text{mer-}\kappa\text{C},\text{N},\text{C}'\text{-}(3,4,5\text{-}(\text{F})_3\text{-C}_6\text{H-2-yl})\text{CH}_2\text{N-CH}(3,4,6\text{-}(\text{F})_3\text{-C}_6\text{H-2-yl})\}\text{Fe}(\text{PMe}_3)_3$  (**1b**) and the generation of ammonia and dihydrogen complexes  $\text{trans-}\{\text{mer-}\kappa\text{C},\text{N},\text{C}'\text{-}(3,4,5\text{-}(\text{F})_3\text{-C}_6\text{H-2-yl})\text{CH}_2\text{N-CH}(3,4,6\text{-}(\text{F})_3\text{-C}_6\text{H-2-yl})\}\text{Fe}(\text{PMe}_3)_2\text{L}$  ( $\text{L} = \text{H}_2$ , **5b**;  $\text{L} = \text{NH}_3$ , **6b**) via **2b**. The dinitrogen, ammonia, and dihydrogen<sup>113–115</sup> complexes all had similar relative free energies, with the  $\text{PMe}_3$  complex about 1.6 kcal/mol above the dinitrogen complex.

Dihydrogen complex **5b** was characterized by a broad triplet ( $J_{\text{PH}} = 12$  Hz) at  $\delta -13.88$  in its  $^1\text{H}$  NMR spectrum. Variable-temperature  $T_1$  measurements were conducted in toluene- $d_8$ , and the  $T_1(\text{min})$  value was found at 228 K, ordering an  $r(\text{H-}$

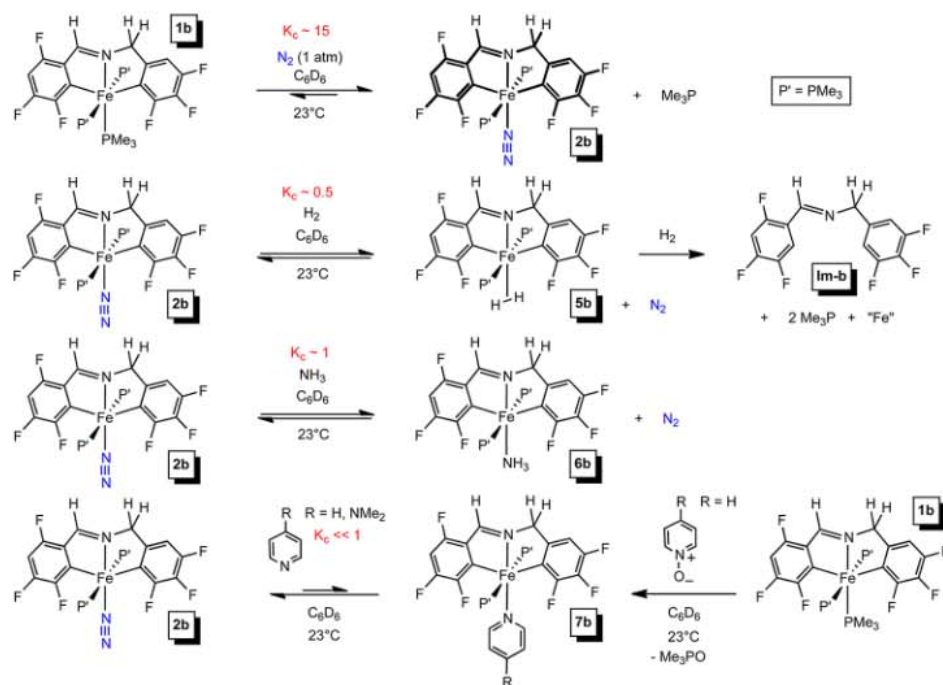
$\text{H})$  value of 0.77 Å,<sup>115–117</sup> assuming rapid rotation of the dihydrogen unit. The dihydrogen complex could not be isolated, due to a slow process that leads to hydrogenation of the Fe–Ar bonds and production of **Im-b** along with the release of  $\text{PMe}_3$ .

Ammonia adduct **6b** was isolated in 98% yield as a purple solid after repeated exposure of **2b** to  $\text{NH}_3$  in benzene. Pyridine derivatives could not be obtained from the addition of  $\text{RC}_6\text{H}_4\text{N}$  to **2b**, but **1b** was treated with pyridine  $N$ -oxide to provide **7b** ( $\text{L} = \text{py}$ ); this was subsequently shown to be unstable under  $\text{N}_2$ , and conditions could not be found to measure a  $K_c$ . Pyridine adduct **7b** was isolated in 70% from **1b** generated in situ from  $(\text{Me}_3\text{P})_4\text{FeMe}_2$  and **Im-b**, and was obtained as red microcrystals.

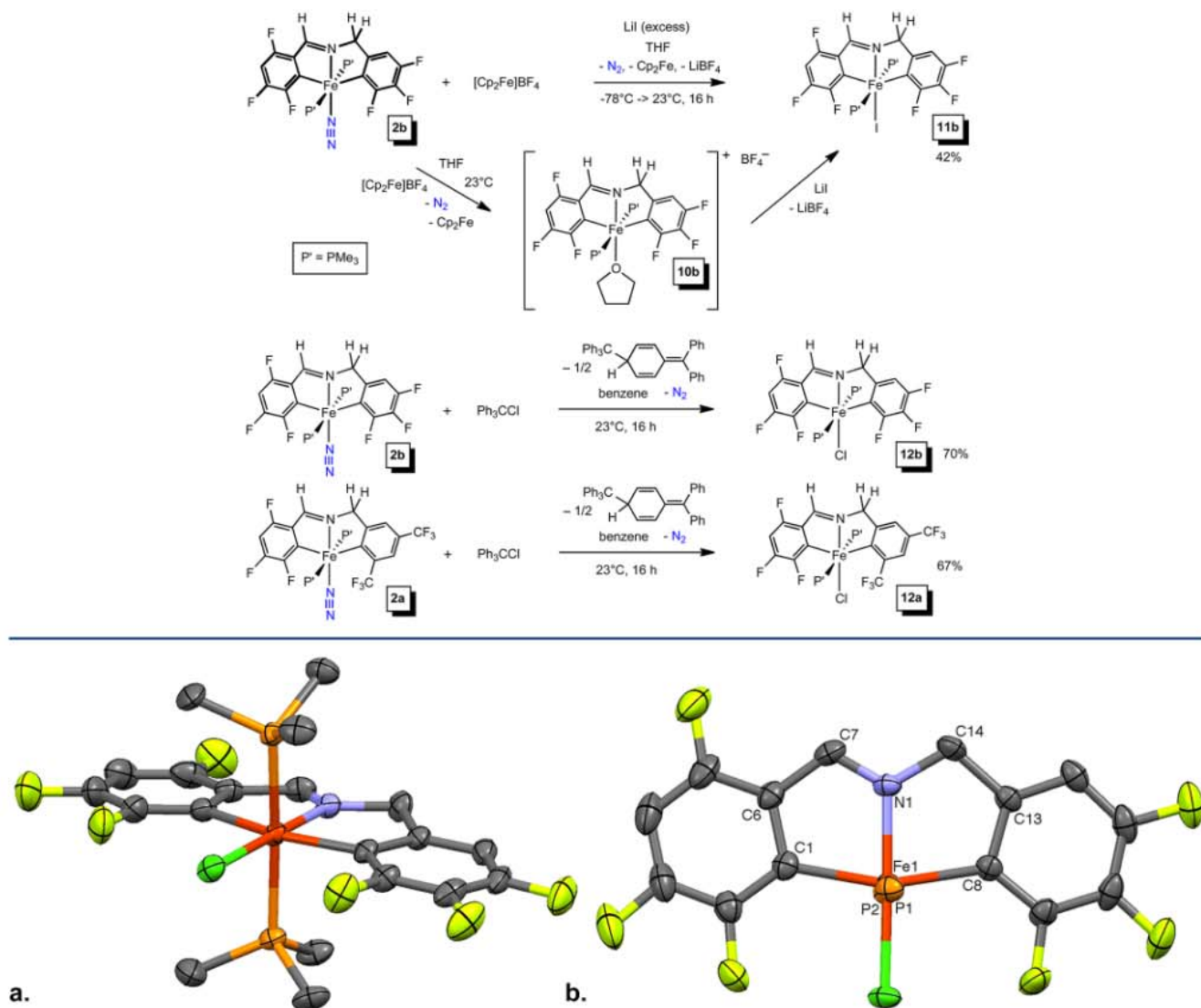
**3. Related Adducts.** Attempts to utilize the diarylimine bisphosphine Fe(II) platform to generate double bonds was successful in regard to  $\pi$ -back-bonding, as dinitrogen, carbonyl, and isocyanide complexes have revealed. The red-brown methyl isocyanide complex **8b** ( $\nu(\text{CN})$  2073  $\text{cm}^{-1}$ ), shown in eq 8, was



Scheme 2



Scheme 3



**Figure 3.** (a) Molecular view (50% probability ellipsoids) of *trans*- $\{\text{mer-}\kappa\text{C},\text{N},\text{C}'\text{-}(3,4,5\text{-}(\text{F})_3\text{-C}_6\text{H-2-yl})\text{CH}_2\text{N-CH}(3,4,6\text{-}(\text{F})_3\text{-C}_6\text{H-2-yl})\}\text{Fe}(\text{PMe}_3)_2\text{Cl}$  (**12b**) and (b) a view down the P–Fe–P axis with the phosphine methyl groups removed. Selected bond distances (Å) and angles (deg): Fe–C1, 2.031(2); Fe–C8, 2.028(2); Fe–N1, 1.9389(17); Fe–Cl, 2.2306(6); Fe–P1, 2.2602(6); Fe–P2, 2.2463(6); N1–C7, 1.299(3); N1–C14, 1.460(3); C6–C7, 1.434(3); C13–C14, 1.497(3); N1–Fe–Cl, 178.04(5); C1–Fe–C8, 160.70(9); P1–Fe–P2, 174.29(2); N1–Fe–C1, 79.80(8); N1–Fe–C8, 80.96(8); N1–Fe–P1, 91.90(5); N1–Fe–P2, 93.74(5); Cl–Fe–P1, 86.64(2); Cl–Fe–P2, 87.75(2); C1–Fe–P1, 89.88(6); C8–Fe–P1, 89.23(6); C1–Fe–P2, 92.02(6); C8–Fe–P2, 90.74(6); C1–Fe–Cl, 98.88(7); C8–Fe–Cl, 100.31(6); Fe–C1–C2, 133.60(18); Fe–C1–C6, 111.90(16); Fe–C8–C9, 131.47(16); Fe–C8–C13, 114.41(15).

prepared in 69% yield. Unfortunately, the generation of Fe(IV) species where the sixth ligand is a  $\pi$  donor has not met with much success. Azide and diazo reagents<sup>64</sup> did not react with dinitrogen complexes under mild conditions, and higher temperatures resulted in degradation. Only in the case of diphenyldiazomethane was a dark purple product isolated, and its spectral characteristics were consistent with an adduct,<sup>118</sup> *trans*- $\{\text{mer-}\kappa\text{C},\text{N},\text{C}'\text{-}(3,4,5\text{-}(\text{F})_3\text{-C}_6\text{H-2-yl})\text{CH}_2\text{N-CH}(3,4,6\text{-}(\text{F})_3\text{-C}_6\text{H-2-yl})\}\text{Fe}(\text{PMe}_3)_2(\text{NN-CPh}_2)$  (**9b**, 76%, eq 9).


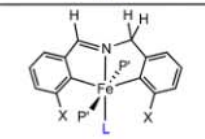

**Oxidations to Fe(III) Complexes.** 1. *Outer-Sphere eT.* Fe(III) species containing metal–carbon bonds are still relatively uncommon,<sup>98</sup> and no Fe(III) derivative has been shown to bind dinitrogen; hence, 1e oxidations of the dinitrogen complexes were explored, as shown in Scheme 3. Oxidation of *trans*- $\{\kappa\text{C},\text{N},\text{C}'\text{-}(3,4,5\text{-}(\text{F})_3\text{-C}_6\text{H-2-yl})\text{CH}_2\text{N-}$

$\text{CH}(3,4,6\text{-}(\text{F})_3\text{-C}_6\text{H-2-yl})\}\text{Fe}(\text{PMe}_3)_2(\text{N}_2)$  (**2b**) with  $[\text{Cp}_2\text{Fe}]\text{-BF}_4$  in the presence of Lil caused the release of  $\text{N}_2$ , and the ferric iodide complex *trans*- $\{\kappa\text{C},\text{N},\text{C}'\text{-}(3,4,5\text{-}(\text{F})_3\text{-C}_6\text{H-2-yl})\text{-CH}_2\text{N-CH}(3,4,6\text{-}(\text{F})_3\text{-C}_6\text{H-2-yl})\}\text{Fe}(\text{PMe}_3)_2\text{I}$  (**11b**) was isolated as a dark green solid in 42% yield. When the oxidation was conducted in the absence of Lil, the red solution darkened but there was no precipitate and no indication of  $\nu(\text{NN})$  in the IR spectrum of the solution. A subsequent addition of Lil generated **11b**; thus, it is likely that the THF adduct **10b** was the initial product in this sequence.

2. *Inner-Sphere eT.* While the iodide complex **11b** was generated via outer-sphere electron transfer (eT), the plausible lability of the dinitrogen in the ferrous  $\text{N}_2$  complexes suggested that inner-sphere paths were also available. Inner-sphere metal-based reagents capable of reacting in nonpolar media are



Table 3. Calculated (M06/6-311+G(d)) Binding Energies for *trans*-{*mer*- $\kappa$ C,N,C'-(3,4,5-(F)<sub>3</sub>-C<sub>6</sub>H-2-yl)CH<sub>2</sub>N-CH(3,4,6-(F)<sub>3</sub>-C<sub>6</sub>H-2-yl)}Fe(PMe<sub>3</sub>)<sub>2</sub> (1 b) + L (L = N<sub>2</sub>, NH<sub>3</sub>, PMe<sub>3</sub>, H<sub>2</sub>) and Related Reactions (P = PMe<sub>3</sub>)

| compound  | L                          | $\Delta H^\circ_{\text{calc}}$<br>(kcal/mol) | $\Delta S^\circ_{\text{calc}}$<br>(eu) | $\Delta G^\circ_{\text{calc}}$ (298 K)<br>(kcal/mol) | $\Delta G^\circ_{\text{calc}}$ (298 K)<br>(kcal/mol) | $\Delta\Delta G^\circ_{\text{exp}}$ (298 K)<br>(kcal/mol) |
|---|----------------------------|--|--|--|--|---|
|  | N <sub>2</sub> <b>2b</b>   | -27.6  | -43.0                                  | -14.8  | 2.6  | 0.0   |
|   | NH <sub>3</sub> <b>6b</b>  | -31.2  | -46.3                                  | -17.4  | 0.0  | 0.0   |
|   | PMe <sub>3</sub> <b>3b</b> | -27.2  | -59.5                                  | -9.4   | 8.0  | 1.6   |
|   | H <sub>2</sub> <b>5b</b>   | -18.6  | -37.0                                  | -7.5   | 9.9  | 0.4   |
|  | N <sub>2</sub> <b>2g</b>   | -30.5  | -37.3                                  | -19.4  |  |   |
|   |                            |  |  |  |  |   |
|  | N <sub>2</sub> X = H       | -31.6  | -37.6                                  | -20.4  | 0.0  |   |
|   | N <sub>2</sub> X = F       | -26.0  | -45.0                                  | -12.6  | 7.8  |   |

uncommon; therefore, Ph<sub>3</sub>CCl was used to convert **2b** and *trans*-{ $\kappa$ C,N,C'-(3,5-(CF<sub>3</sub>)<sub>2</sub>-C<sub>6</sub>H<sub>2</sub>-2-yl)CH<sub>2</sub>N-CH(3,4,6-(F)<sub>3</sub>-C<sub>6</sub>H-2-yl)}Fe(PMe<sub>3</sub>)<sub>2</sub>(N<sub>2</sub>) (**2a**) to their corresponding Fe(III) chloride derivatives **12b** and **12a**, respectively, in very good yields. Each halide complex had a tractable <sup>1</sup>H NMR spectrum, and Evans method<sup>104</sup> measurements showed each to have an *S* = 1/2 ground state with a significant spin-orbit contribution:<sup>105</sup> **11b**,  $\mu_{\text{eff}} = 2.0(1) \mu_{\text{B}}$ ; **12b**,  $\mu_{\text{eff}} = 2.0(1) \mu_{\text{B}}$ ; **12a**,  $\mu_{\text{eff}} = 2.1(1) \mu_{\text{B}}$ .

**3. Structure of *trans*-{ $\kappa$ C,N,C'-(3,4,5-(F)<sub>3</sub>-C<sub>6</sub>H-2-yl)CH<sub>2</sub>N-CH(3,4,6-(F)<sub>3</sub>-C<sub>6</sub>H-2-yl)}Fe(PMe<sub>3</sub>)<sub>2</sub>Cl (**12b**).** Selected crystallographic and refinement data pertaining to the X-ray structure of *trans*-{ $\kappa$ C,N,C'-(3,4,5-(F)<sub>3</sub>-C<sub>6</sub>H-2-yl)CH<sub>2</sub>N-CH(3,4,6-(F)<sub>3</sub>-C<sub>6</sub>H-2-yl)}Fe(PMe<sub>3</sub>)<sub>2</sub>Cl (**12b**) are given in Table 2, and views of the molecule are provided in Figure 3. The iron-imine distance of 1.9389(17) Å is essentially the same as in **2b**, while the iron-carbon bonds are slightly longer (0.02–0.04 Å) at 2.031(2) and 2.028(2) Å, as are the *d*(Fe–P) values of 2.2602(6) and 2.2463(6) Å. It is plausible that the contraction of the 3d orbitals upon oxidation, while typically causing shorter bond distances in molecules with greater ionic character, renders covalent interactions longer due to decreased orbital overlap.<sup>98</sup> As the Fe–Ar distances increase, the bite angle of the diarylimine ligand decreases to 160.70(9)°, and the related N1–Fe–C(Ar) angles are 79.80(8) and 80.96(8)°, while their complementary C1–Fe–Cl and C8–Fe–Cl angles are 98.88(7) and 100.31(6)°, respectively. Remaining core angles among adjacent ligands average 90.2(23)°, and the N1–Fe–Cl and P1–Fe–P2 angles are 178.04(5) and 174.29(2)°, respectively; hence, the core is very similar to that of **2b**.

## DISCUSSION

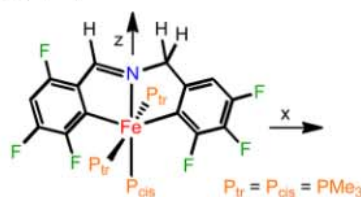
**Relative Binding Energies.** In order to assess the steric and electronic factors present in diarylimine **1b**, calculations on the binding energies of L (L = N<sub>2</sub>, NH<sub>3</sub>, PMe<sub>3</sub>, H<sub>2</sub>) to the putative  $\nu$ -coordinate *trans*-{*mer*- $\kappa$ C,N,C'-(3,4,5-(F)<sub>3</sub>-C<sub>6</sub>H-2-yl)CH<sub>2</sub>N-CH(3,4,6-(F)<sub>3</sub>-C<sub>6</sub>H-2-yl)}Fe(PMe<sub>3</sub>)<sub>2</sub> (**1b**) were conducted, and the results are given in Table 3. Initial efforts utilizing B3LYP ran counter to the experimental observations, and a switch to the M06<sup>119</sup>/6-311+G(d)<sup>120</sup> functional<sup>121</sup> was rationalized on the basis of the need for better calculations of van der Waals interactions: i.e., the sterics of binding. The calculations are reasonable, showing that N<sub>2</sub> and NH<sub>3</sub> bind

similarly, while binding of PMe<sub>3</sub> and H<sub>2</sub> is significantly less favorable. With respect to the experimental relative binding studies, dihydrogen is the outlier, as it is calculated to be 9.9 kcal/mol less favorable than N<sub>2</sub> binding, while experimentally it is found to be roughly equal to N<sub>2</sub> and NH<sub>3</sub>. Dinitrogen and dihydrogen are often found to be comparable ligands.<sup>113–115</sup> PMe<sub>3</sub> is unfavorable, and the calculation again appears to overestimate its relative binding energy. A closer look at free energies of binding pertaining to N<sub>2</sub> vs PMe<sub>3</sub> reveals the difference to be entropic in origin, as the relative binding of PMe<sub>3</sub> manifests a  $\Delta S^\circ$  value of 16.5, which can be construed as reflecting the heavy steric penalty as the phosphine abuts the *o*-fluorine substituents.

The binding assessments continued with a calculation of dinitrogen binding to *trans*-{*mer*- $\kappa$ C,N,C'-(4,5,6-(F)<sub>3</sub>-C<sub>6</sub>H-2-yl)CH<sub>2</sub>N-CH(4,5,6-(F)<sub>3</sub>-C<sub>6</sub>H-2-yl)}Fe(PMe<sub>3</sub>)<sub>2</sub> (**1g**), which does not contain *o*-fluorines. The binding of N<sub>2</sub> to this  $\nu$ -coordinate fragment ( $\Delta G^\circ_{\text{calc}} = -19.4$  kcal/mol) was calculated to be enthalpically (–2.9 kcal/mol) and entropically (5.7 eu) more favorable than to **1b** ( $\Delta G^\circ_{\text{calc}} = -14.8$  kcal/mol), a clear indication of how the *o*-fluorines inductively destabilize dinitrogen binding and have a deleterious entropic effect (*d*(*o*-F...N<sub>bnd</sub>) = 2.9 Å; *d*(*o*-F...N<sub>term</sub>) = 3.1 Å) on even a linear ligand such as N<sub>2</sub>. In order to make sure these arguments are not compromised by the unique dispositions of the fluorine substituents in **2b,g**, the hypothetical unsubstituted diarylimine iron dinitrogen complex was compared to one containing just two *o*-fluorines, and the results are quite similar.

**Spin State of (diarylimine)Fe(PMe<sub>3</sub>)<sub>3</sub> (**1a–g**).** The precursors to the dinitrogen complexes, tris-phosphine species {*mer*- $\kappa$ C,N,C'-(Ar-2-yl)CH<sub>2</sub>N-CH(Ar-2-yl)}Fe(PMe<sub>3</sub>)<sub>3</sub> (**1a–f**), were shown to be diamagnetic when the diarylimine ortho substituents were two fluorines (**1b**) or one methoxide (**1d**). Paramagnetic properties (*S* = 1) were observed for diarylimine ortho substituents that were one fluorine and one CF<sub>3</sub> (**1a**), one CF<sub>3</sub> (**1c**), and one methyl group (**1e,f**). Since a methoxy group can be considered smaller than a methyl due to its orientation, a correlation between paramagnetism and larger substituents exists, highlighting the influence of steric features on electronic structure.

Calculations on {*mer*- $\kappa$ C,N,C'-(3,4,5-(F)<sub>3</sub>-C<sub>6</sub>H-2-yl)CH<sub>2</sub>N-CH(3,4,6-(F)<sub>3</sub>-C<sub>6</sub>H-2-yl)}Fe(PMe<sub>3</sub>)<sub>3</sub> (**1b**) were con-

Table 4. Calculated Metric Parameters for the Singlet, Triplet, and Quintet States of  $\{mer\text{-}C,N,C'-(3,4,5\text{-}(F)_3\text{-}C_6H\text{-}2\text{-}yl)CH_2N\text{-}CH(3,4,6\text{-}(F)_3\text{-}C_6H\text{-}2\text{-}yl)\}Fe(PMe_3)_3$  (**1b**)

|                                  | spin state             |                        |                        |
|----------------------------------|------------------------|------------------------|------------------------|
|                                  | S = 0                  | S = 1                  | S = 2                  |
| $d(Fe-C)$ (Å)                    | 2.07, 2.08             | 2.04, 2.06             | 2.20, 2.21             |
| $d(Fe-P_{tr})$ (Å)               | 2.26, 2.29             | 2.26, 2.26             | 2.57, 2.59             |
| $d(Fe-P_{cis})$ (Å)              | 2.36                   | 3.18                   | 2.69                   |
| $d(Fe-N)$ (Å)                    | 1.97                   | 2.15                   | 2.20                   |
| $\angle C-Fe-C$ (deg)            | 159.7                  | 155.8                  | 150.8                  |
| $\angle C-Fe-N$ (deg)            | 80.1, 80.1             | 77.9, 77.9             | 75.2, 75.7             |
| $\angle P_{tr}-Fe-P_{cis}$ (deg) | 89.6, 93.6             | 87.0, 87.0             | 89.5, 91.0             |
| $\angle P_{tr}-Fe-P_{tr}$ (deg)  | 173.8                  | 172.8                  | 176.9                  |
| $\angle P_{tr}-Fe-N$ (deg)       | 86.6, 90.7             | 93.1, 93.4             | 88.7, 91.1             |
| $\angle P_{cis}-Fe-N$ (deg)      | 173.5                  | 175.8                  | 174.9                  |
| $\angle P_{tr}-Fe-C$ (deg)       | 85.9, 88.2, 90.5, 94.5 | 89.1, 89.4, 92.2, 92.2 | 87.9, 89.1, 91.3, 91.6 |
| $\angle P_{cis}-Fe-C$ (deg)      | 95.1, 105.1            | 97.9, 106.2            | 99.7, 109.5            |
| $E_{rel}$ (kcal/mol)             | -7.0                   | -3.0                   | 0.0                    |
| $H_{rel}$ (kcal/mol)             | -4.7                   | -2.3                   | 0.0                    |
| $G_{rel}$ (kcal/mol)             | 3.9                    | 2.3                    | 0.0                    |

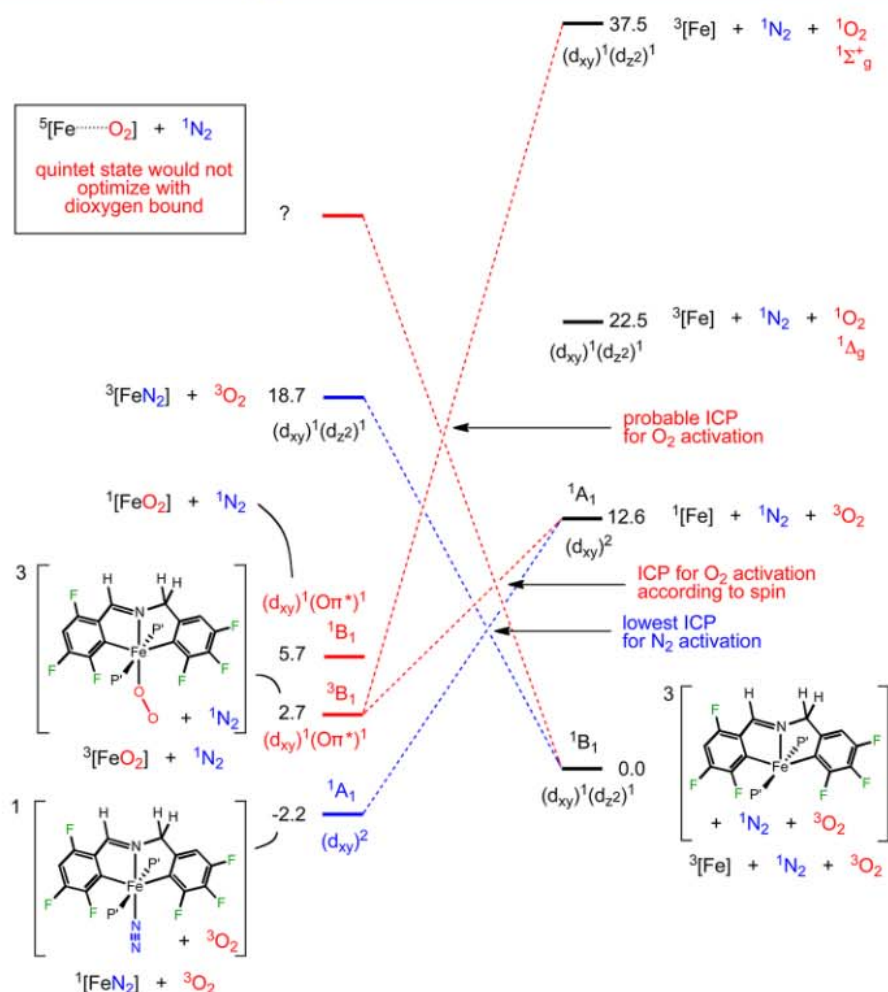
ducted for  $S = 0, 1, 2$ , and the metric parameters and energies of these spin states are given in Table 4. There is a general lengthening of bond distances from singlet to triplet to quintet and a corresponding change in bond angles. Although the observed GS of **1b** is  $S = 0$ , the singlet state is calculated to be 1.8 kcal/mol above the triplet state ( $(d_{xy})^1(d_z)^1$ ) in free energy and 3.9 kcal/mol above the quintet state ( $(d_{yz})^2(d_{xz})^1(d_{xy})^1(d_z)^1(d_x^2-y^2)^1$ ). While the calculated free energies obviously do not conform to experiment, the  $E_{rel}$  and  $H_{rel}$  values parallel the experimental observations, at least in terms of predicting diamagnetic behavior. Relative energy calculations of comparative closed-shell vs open-shell systems can present problems for density functional methods;<sup>106–108</sup> hence, the important outcome of the calculations is the relatively similar values of the three states. Moreover, the calculated entropic corrections, which the calculations suggest are responsible for tipping the free energy balance toward the high-spin state, may be exaggerated in a gas-phase calculation.

The Fe–P bond distances of the phosphine opposite the imine–N change dramatically from  $S = 0$  (2.36 Å) to the  $S = 1$  (3.18 Å) state as  $d_z^2$  becomes half-occupied, while the  $d(Fe-P_{tr})$  values remain the same. Since the calculated GS of the putative  $\nu$ -coordinate intermediate, **1b**, is a triplet, intersystem crossing from **1b** to **1b** probably occurs smoothly as the iron–phosphine bond is elongated, and the barrier to  $PMe_3$  loss is likely to be close to the calculated binding free energy of 8.0 kcal/mol. A similar observation has been made regarding spin state changes in dinitrogen bonding to related Fe(II) compounds.<sup>95</sup>

**Origin of the Selectivity of  $N_2$  Extraction over  $O_2$  from Air.** The selectivity for binding dinitrogen over dioxygen to a  $\nu$ -coordinate fragment such as  $trans\text{-}\{mer\text{-}C,N,C'-(3,4,5\text{-}(F)_3\text{-}C_6H\text{-}2\text{-}yl)CH_2N\text{-}CH(3,4,6\text{-}(F)_3\text{-}C_6H\text{-}2\text{-}yl)\}Fe(PMe_3)_2$

(**1b**) appears to be kinetic in origin, since prolonged exposure of the  $N_2$  complexes to  $O_2$  causes degradation, and no clean dioxygen complexes were identified. In addition, exposure of **1b** to  $O_2$  produced  $Me_3PO$  and a black solid, consistent with irreversible  $O_2$  binding and subsequent decomplexation. Recall that stability in air is significant, even in the worst cases, implicating reversible trapping by dinitrogen and irreversible destruction by dioxygen.

The results of calculations on the binding of  $N_2$  vs  $O_2$  to  $trans\text{-}\{mer\text{-}C,N,C'-(3,4,5\text{-}(F)_3\text{-}C_6H\text{-}2\text{-}yl)CH_2N\text{-}CH(3,4,6\text{-}(F)_3\text{-}C_6H\text{-}2\text{-}yl)\}Fe(PMe_3)_2$  (**1b**) are provided in Figure 4, and some insights are illustrated, albeit with certain assumptions. First, note that the  $N_2$  complex, in short form denoted as  $^1[FeN_2]$ , is calculated to be 2.7 kcal/mol more stable than a dioxygen complex that is best construed as a ferric superoxide species,  $^3[FeO_2]$  or  $^3[Fe^{III}(O_2^-)]$ . In order to produce either species, the  $\nu$ -coordinate precursor  $^3[Fe]$  (i.e., **1b**) must intersystem cross, since it possesses a triplet ground state (GS) that is  $(d_{xy})^1(d_z)^1$ , which can be thought of in orbital symmetry terms as a  $\pi^1\sigma^1$ . The product  $^1[FeN_2]$  has an abbreviated electron configuration of  $(d_{xz})^2(N\sigma)^2$  which is essentially  $\pi^2\sigma^2$ ; hence, the conversion of **1b** +  $N_2$  ( $\pi^1\sigma^1 + \sigma^2$ ) to **2b** is not orbital symmetry allowed, nor is it spin allowed. The GS of  $^3[Fe] + ^1N_2$  correlates to an excited state (ES) on the bound substrate side (left) of Figure 4 that is 20.9 kcal/mol above  $^1[FeN_2]$ . The  $^1[Fe]$  or  $(d_{xz})^2$  configuration of **1b** is only 12.6 kcal/mol above the GS, and the intersystem crossing point (ICP) to a  $^1[FeN_2]$  ( $^1[FeN_2]$ ) from **1b** ( $^3[Fe] + ^1N_2$ ) is the lowest for either substrate, requiring only the conversion of HS Fe(II) to LS Fe(II) as the main electronic obstacle to surmount. Cases of  $N_2$  bonding that incur an intersystem crossing event have been similarly rationalized.<sup>95–97</sup>



**Figure 4.** Correlation diagram for the binding of dinitrogen vs dioxygen to *ve*-coordinate *trans*-{*mer*- $\kappa$ C,N,C'-(3,4,5-(F)<sub>3</sub>-C<sub>6</sub>H-2-yl)CH<sub>2</sub>NCH(3,4,6-(F)<sub>3</sub>-C<sub>6</sub>H-2-yl)}Fe(PMe<sub>3</sub>)<sub>2</sub> (**1 b**), showing the lower intersystem crossing point (ICP) for the former. Since the quintet state of the bound O<sub>2</sub> complex was not located, the ICP for dioxygen binding is somewhat arbitrary; see the text for a discussion of its placement.

The binding of dioxygen to GS **1 b** ( $^3[\text{Fe}] + ^3\text{O}_2$ ) is complicated, in part due to the inability to locate a geometry pertaining to an O<sub>2</sub>-bound quintet state to which it would correlate. The GS may thus be construed as  $(d_{xy})^1(d_{z^2})^1 + \pi^{*1}\pi^{*1}$ , and its conversion to the Fe(III) superoxide species  $^3[\text{FeO}_2]$  ( $(d_{xy})^1(\text{O}\sigma)^2(\text{O}\pi)^1$ ) is slightly endergonic (+2.7 kcal/mol). No steric interference to dioxygen binding was noted in the calculations; hence, the additional thermodynamic preference for dinitrogen binding stems purely from electronic factors. It is plausible that the strong field imparted by the phosphines and diaryl ligands renders the ferrous centers less susceptible to oxidation and thus endergonic with respect to the calculated Fe(III) superoxide. While the lowest spin state correlation occurs from  $^1[\text{Fe}] + ^3\text{O}_2$  at 12.6 kcal/mol, the orbital symmetry of this state, which is  $(d_{xz})^2(\pi^*\pi^*)$  or  $(\pi^2)(\pi^*\pi^*)$ , does not correlate with the orbital symmetry of the bound-O<sub>2</sub> GS. It also seems unlikely that the ICP derived from this spin correlation would serve to significantly differentiate between N<sub>2</sub> and O<sub>2</sub> because it is likely to be only slightly higher than the ICP for dinitrogen binding, although it is highly dependent on where and if a suitable quintet surface exists. This lowest O<sub>2</sub>-bound state best correlates with a high-energy  $^3[\text{Fe}] + ^1\text{O}_2$  state in which the singlet oxygen  $^1(\pi^{*1}\pi^{*})$  configuration ( $^1\Sigma^+$ ) can be considered  $(\pi^{*1}\sigma^1)$  along the reaction coordinate.

A simple pairing of the Fe( $(d_{z^2})^1$ ) and O( $\sigma^1$ ) spins orders the calculated ground-state Fe(III) superoxide species  $^3[\text{FeO}_2]$  ( $(d_{xz})^1(\text{O}\sigma)^2(\text{O}\pi)^1$ ). The ICP that arises from this correlation is significantly higher than that for N<sub>2</sub>, which accounts for the N<sub>2</sub> vs O<sub>2</sub> selectivity, but its value is again dependent on the nature of the quintet surface.

In summary, while the  $^1[\text{FeN}_2]$  complex (e.g., **2b**) is 4.9 kcal/mol below the calculated first-formed dioxygen adduct, there is a significantly greater kinetic preference for N<sub>2</sub> binding. The kinetic preference likely stems from both spin and orbital symmetry constraints. A quintet surface that would correlate directly with the reactant  $^3[\text{Fe}] + ^3\text{O}_2$  surface has not been located and may indicate that  $^3\text{O}_2$  cannot bind to  $^3[\text{Fe}]$ ; such an adduct would not optimize. This is not surprising, because an octahedral Fe(II) center that is  $S = 1$  would have an electron in a  $\sigma^*$  orbital and would likely be unstable relative to an electron transfer to a low-energy ferric state and O<sub>2</sub><sup>-</sup>. It is precisely such an event that would lead to the calculated superoxide product, but finding this ICP without a ready correlation is difficult. The orbital symmetry of the calculated superoxide complex denoted as  $^3[\text{FeO}_2]$  correlated with a high-energy reagent surface; hence, it is quite likely that the ICP is high in energy. Since a dioxygen adduct could not be isolated or observed spectroscopically due to rapid degradation, this

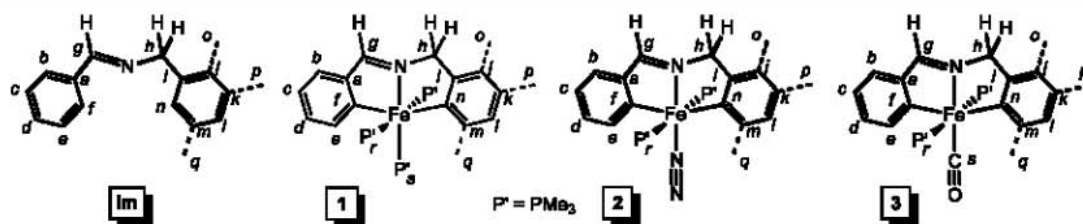


Figure 5. Key for  $^1\text{H}$ ,  $^{13}\text{C}\{^1\text{H}\}$ ,  $^{31}\text{P}$ , and  $^{19}\text{F}$  NMR assignments.

analysis is predicated on the calculated initially formed dioxygen species, the Fe(III) superoxide  $^3[\text{FeO}_2]$ .

## CONCLUSIONS

Due to steric interactions, ortho-substituted diarylimine ligands cause ready dissociation of  $\text{PMe}_3$  from  $\{\text{mer-}\kappa\text{C},\text{N},\text{C}'\text{-(Ar-2-yl)}\}\text{CH}_2\text{N-CH(Ar-2-yl)}\}\text{Fe}(\text{PMe}_3)_3$  (**1a–f**) complexes, and the resulting  $\nu$ -coordinate species,  $\{\text{mer-}\kappa\text{C},\text{N},\text{C}'\text{-(Ar-2-yl)}\}\text{CH}_2\text{N-CH(Ar-2-yl)}\}\text{Fe}(\text{PMe}_3)_2$  (**1a–f**), selectively extract dinitrogen from air. The compounds eventually degrade, rapidly in wet air due to irreversible protonation reactions, but far less swiftly in dry air, where the selective recombination of **1a–f** and dinitrogen renders the systems significantly stable in the presence of dioxygen. Calculations show the dinitrogen complexes  $\{\text{mer-}\kappa\text{C},\text{N},\text{C}'\text{-(Ar-2-yl)}\}\text{CH}_2\text{N-CH(Ar-2-yl)}\}\text{Fe}(\text{PMe}_3)_2\text{N}_2$  (**2a–f**) are kinetically and thermodynamically preferred over the *calculated* dioxygen adduct, a ferric superoxide, while experiments are consistent with rapid degradation of the iron organometallic species subsequent to dioxygen binding. Dinitrogen, ammonia, and dihydrogen bind similarly to the  $\nu$ -coordinate species **1b**, while  $\text{PMe}_3$  and pyridine are disfavored, principally due to the aforementioned steric features. Ligands with  $\pi$ -accepting capability bind strongly, but formation of iron multiple bonds could not be effected. Ferric derivatives generated via inner (**2a,b**) and outer-sphere oxidations of (**2b**) do not bind  $\text{N}_2$ . It is conceivable that a chemical means to remove dinitrogen from hydrocarbon feed streams can be designed on the basis of the principles discovered, even with trace dioxygen present. Furthermore, perhaps the  $\mu_6$ -carbide present in the operational cluster of nitrogenase, i.e.,  $[(\text{Cys})\text{Fe}(\mu_3\text{-S})_3\text{Fe}_3(\mu\text{-S})_3(\mu_6\text{-C})\text{Fe}_3(\mu_3\text{-S})_3\text{Mo}(\text{His})(\text{Homocitrate}))^n]^{122}$  helps impart a strong field and an electronic influence on dinitrogen bonding, akin to the species herein.

## EXPERIMENTAL SECTION

**General Considerations.** Since a number of the preparations pertaining to different diarylimine complexes are repetitive, this section focuses on those pertaining to **Im-b**. For the remaining complexes and spectral data, see the Supporting Information.

All manipulations were performed using either glovebox or high-vacuum-line techniques. Hydrocarbon solvents containing 1–2 mL of added tetraglyme and etheral solvents were distilled under nitrogen from purple sodium benzophenone ketyl and vacuum-transferred from the same prior to use. Benzene- $d_6$  and toluene- $d_8$  were dried over sodium, vacuum-transferred, and stored under  $\text{N}_2$ . THF- $d_8$  was dried over sodium benzophenone ketyl. Methylene chloride- $d_2$  was dried over  $\text{CaH}_2$ , vacuum-transferred and stored over activated 4 Å molecular sieves.  $\text{Fe}(\text{PMe}_3)_4\text{Me}_2$  was prepared according to a literature procedure.<sup>99</sup> Compounds **1d,h,i** were previously reported.<sup>98</sup> All other chemicals were commercially available and used as received. All glassware was oven-dried.

NMR spectra (see Figure 5 for assignment key) were obtained using Mercury-300 and INOVA 400, 500, and 600 MHz spectrometers.

Chemical shifts are reported relative to benzene- $d_6$  ( $^1\text{H}$ ,  $\delta$  7.16;  $^{13}\text{C}\{^1\text{H}\}$ ,  $\delta$  128.39), THF- $d_8$  ( $^1\text{H}$ ,  $\delta$  3.58;  $^{13}\text{C}\{^1\text{H}\}$ ,  $\delta$  67.57), and  $\text{CD}_2\text{Cl}_2$  ( $^1\text{H}$ ,  $\delta$  5.32;  $^{13}\text{C}\{^1\text{H}\}$ ,  $\delta$  54.00). Infrared spectra were recorded on a Nicolet Avatar 370 DTGX spectrophotometer interfaced to an IBM PC (OMNIC software). UV–vis spectra were obtained on an Ocean Optics USB2000 spectrometer. Solution magnetic measurements were conducted via the Evans method in benzene- $d_6$ .<sup>104</sup> Elemental analyses were performed by Robertson Microлит Laboratories, Madison, NJ, or Complete Analysis Laboratories, Inc., Parsippany, NJ.

**Procedures.** **1. General Procedure for Synthesis of Imines.** To a suspension of  $\text{MgSO}_4$  (5–8 equiv) in  $\text{CH}_2\text{Cl}_2$  were added 1.5 mmol of aldehyde and 1.5 mmol of amine. After it was stirred for 12 h, the mixture was filtered and concentrated to yield a colorless to pale yellow oil in >98% purity (by  $^1\text{H}$  NMR). All aryl positions are CH unless noted. For **Im-a** and **Im-c–Im-g**, see the Supporting Information.

**Im-b** ( $b = d = e = k = l = m = \text{CF}$ ).  $^1\text{H}$  NMR ( $\text{C}_6\text{D}_6$ , mult,  $J$  (Hz); assign):  $\delta$  7.71 (td, 9, 7; c), 6.24 (td, 10, 6; f), 7.98 (s, g), 3.91 (s, h), 6.51 (dd, 8, 7; j, n).  $^{13}\text{C}\{^1\text{H}\}$  NMR ( $\text{C}_6\text{D}_6$ , mult,  $J_{\text{CF}}$  (Hz); assign):  $\delta$  135.89 (a), 157.63 (d, 250; b), 105.89 (d, 250; c), 151.63 (d, 250; d), 152.37 (d, 250; e), 115.25 (f), 153.35 (g), 62.91 (h), 120.47 (i), 111.64 (j, n), 147.70 (d, 250; k, m), 139.02 (d, 250; l).  $^{19}\text{F}$  NMR ( $\text{C}_6\text{D}_6$ , mult,  $J$  (Hz); assign):  $\delta$  -123.84 (ddd, 16, 11, 6; b), -128.48 (dtd, 22, 9, 5; d), -134.76 (dd, 21, 8; m, k), -141.26 (tdd, 20, 14, 7; e), -163.20 (tt, 21, 7; l).

**2. General Procedure for Tris- $\text{PMe}_3$  Complexes.** Since **1a–f** cannot be exposed to dinitrogen, spectral assays of the (diarylimine)Fe( $\text{PMe}_3$ )<sub>3</sub> complexes were conducted on NMR tube scale reactions. In a typical reaction, ~8 mg (0.020 mmol) of  $(\text{Me}_3\text{P})_4\text{FeMe}_2$  and 0.020 mmol of imine were loaded into a J. Young NMR tube into which ~0.6 mL of  $\text{C}_6\text{D}_6$  was vacuum-transferred. The reactions went to completion in 1–6 h, and the contents were never exposed to dinitrogen. Evans method measurements were conducted on the crude paramagnetic compounds generated *in situ*. For **1c–f**, see the Supporting Information.

**1a** ( $b = d = e = \text{CF}$ ,  $kp = mq = \text{CCF}_3$ ).  $^1\text{H}$  NMR ( $\text{C}_6\text{D}_6$ ):  $\delta$  66.13 (2H), 34.01 (2H), 32.57 (2H), -4.86 (18H), -11.46 (9H). Free  $\text{PMe}_3$  was noted at  $\delta$  0.80.  $^{31}\text{P}\{^1\text{H}\}$  NMR ( $\text{C}_6\text{D}_6$ ):  $\delta$  -60.0 (br s, free  $\text{PMe}_3$ ); no other resonances were noted.  $\mu_{\text{eff}}(296 \text{ K}) = 3.0, 3.3 \mu_{\text{B}}$ .

**1b** ( $b = d = e = k = l = m = \text{CF}$ ).  $^1\text{H}$  NMR ( $\text{C}_6\text{D}_6$ , mult, assign):  $\delta$  6.39 (s, c, j), 8.27 (s, g), 4.24 (s, h), 0.46 (s, r), 1.36 (s, s), 13.36 (f), 163.13 (g), 65.59 (h), 111.77 (i), 96.50 (j), 146.44 (d, 250; k), 144.97 (d, 250; l), 157.54 (d, 250; m), 111.26 (n), 16.97 (t, 10; r), 16.08 (d, 13; s).  $^{19}\text{F}$  NMR: ( $\text{C}_6\text{D}_6$ , mult,  $J_{\text{CF}}$  (Hz); assign):  $\delta$  -106.35 (d, 32; m), -147.15 (dd, 30, 8; d), -120.42 (dd, 21, 7; k) -166.60 (dd, 33, 20; p), -116.08 (dd, 25, 10; b), -133.28 (dd, 32, 9; e).  $^{31}\text{P}\{^1\text{H}\}$  NMR ( $\text{C}_6\text{D}_6$ , mult,  $J_{\text{CF}}$  (Hz); assign): 14.14 (d, 58; o), 9.60 (t, 58; p).

**3. General Procedure for Dinitrogen Complexes.** In a 100 mL bomb reactor charged with  $\text{Fe}(\text{PMe}_3)_4\text{Me}_2$  (0.200 g, 1.02 mmol) and imine (1 equiv) was transferred 15 mL of benzene. The mixture was placed under an atmosphere of  $\text{N}_2$  at 23 °C. The solution was stirred for 6 h. Upon removal of solvent, the crude mixture was dissolved in  $\text{Et}_2\text{O}$ , the solution was filtered, and the residue was washed ( $4 \times 10$  mL of  $\text{Et}_2\text{O}$ ). Crystallization from hexanes at -78 °C afforded product. For **2a,c–g**, see the Supporting Information.

**2b** ( $b = d = e = k = l = m = \text{CF}$ ). Dark red crystalline **2b** (0.184 g) was obtained in 67% yield.  $^1\text{H}$  NMR ( $\text{C}_6\text{D}_6$ , mult, assign):  $\delta$  7.79 (s, g), 6.36 (m, c, j), 3.95 (s, h), 0.44 (s, r).  $^{13}\text{C}\{^1\text{H}\}$  NMR ( $\text{C}_6\text{D}_6$ , mult,  $J_{\text{CF}}$  (Hz); assign):  $\delta$  133.26 (a), 160.4 (d, 230; b), 97.34 (c), 157.19 (d, 230; d), 157.93 (d, 230; e), 112.47 (f), 161.98 (g), 64.04 (h), 142.75 (i), 104.45 (j), 148.17 (d, 240; k), 138.46 (d, 240; l), 150.80 (d, 240; m), 111.07 (n), 12.90 (t, 12; r).  $^{19}\text{F}$  NMR ( $\text{C}_6\text{D}_6$ , mult,  $J_{\text{CF}}$  (Hz); assign):  $\delta$  -119.36 (d, 31; m), -145.94 (dd, 19, 11; k), -118.92 (dd, 24, 11; b), -166.13 (dd, 31, 20; l), -128.81 (dd, 30, 25; e), -132.18 (ddd, 30, 10, 3; d).  $^{31}\text{P}\{^1\text{H}\}$  NMR ( $\text{C}_6\text{D}_6$ , mult, assign):  $\delta$  19.95 (s, r).  $^{15}\text{N}$  NMR (**1b**- $^{15}\text{N}_2$ , 60.8 MHz, referenced to  $\text{NH}_3(\text{l})$ ):  $\delta$  334.15 (br d,  $^1J_{\text{N}^{15}\text{N}} = 4$  Hz,  $^3J_{\text{N}^{15}\text{N}} < 1.5$  Hz,  $\text{N}_p$ ), 369.55 (q,  $^1J_{\text{N}^{15}\text{N}} = 5$  Hz,  $^2J_{\text{N}^{15}\text{N}} = 5$  Hz,  $\text{N}_a$ ).  $^{109}\text{Ag}$  IR ( $\text{C}_6\text{D}_6$ ):  $\nu(\text{N}_2)$  2107  $\text{cm}^{-1}$ . Anal. Calcd for  $\text{C}_{20}\text{H}_{23}\text{N}_3\text{F}_6\text{FeP}_2$ : C, 44.72; H, 4.32; N, 7.82. Found: C, 44.85; H, 4.22; N, 7.88.

**4. General Procedure for Carbonyl Complexes.** In a 100 mL bomb reactor charged with  $(\text{PMe}_3)_2\text{FeMe}_2$  (0.100 g, 0.513 mmol) and imine (1 equiv) was transferred 15 mL of benzene at  $-78$  °C. The solution was warmed to  $23$  °C and stirred for 4 h. Upon removal of solvent and excess  $\text{PMe}_3$ , the crude mixture was redissolved in benzene, placed under an atmosphere of dry CO, and stirred for 12 h. Solvent and excess CO was removed from the bomb reactor via vacuum transfer, and the crude solid was dissolved in  $\text{Et}_2\text{O}$ , filtered, and washed ( $3 \times 10$  mL) with  $\text{Et}_2\text{O}$ . Crystallization from hexanes at  $-78$  °C a ordered product. For **3a,c,d,f**, see the Supporting Information.

**3b** ( $b = d = e = k = l = m = \text{CF}$ ). Dark red microcrystals were (0.110 g) isolated in 80% yield.  $^1\text{H}$  NMR ( $\text{C}_6\text{D}_6$ , mult, assign):  $\delta$  6.36 (m, c, j), 7.96 (s, g), 4.18 (s, h), 0.44 (s, r).  $^{13}\text{C}\{^1\text{H}\}$  NMR ( $\text{C}_6\text{D}_6$ , mult,  $J_{\text{CF}}$  (Hz); assign):  $\delta$  149.13 (a), 158.93 (d, 240; b), 97.81 (c), 158.08 (d, 240; d), 154.57 (d, 240; e), 142.67 (f), 160.95 (g), 63.40 (h), 147.26 (i), 104.59 (j), 157.15 (d, 240; k), 151.83 (d, 240; l), 156.24 (d, 240; m), 132.88 (n), 14.72 (t, 13; r), 190.97 (s).  $^{19}\text{F}$  NMR ( $\text{C}_6\text{D}_6$ , mult,  $J_{\text{CF}}$  (Hz); assign):  $\delta$  -110.14 (d, 30; m), -145.40 (dd, 28, 8; k), -118.70 (ddd, 22, 9, 4; b), -120.92 (ddd, 30, 20, 5; e), -165.24 (dd, 31, 22; l), -131.28 (ddd, 30, 10, 4; d).  $^{31}\text{P}\{^1\text{H}\}$  NMR ( $\text{C}_6\text{D}_6$ , mult, assign):  $\delta$  20.54 (s, r). IR ( $\text{C}_6\text{D}_6$ ):  $\nu(\text{CO})$  1936  $\text{cm}^{-1}$ .

**5. trans-[ $\kappa\text{C,N}$ -(3,4,5-( $\text{F}_3\text{-C}_6\text{H}_2$ )/ $\text{CH}_2\text{N}$  CH(3,4,6-( $\text{F}_3\text{-C}_6\text{H}_2$ )-yl)]Fe( $\text{PMe}_3$ ) $_3$ (CCMe)] (**4b-Me**). In a 25 mL round-bottom flask charged with  $\text{Fe}(\text{PMe}_3)_4\text{Me}_2$  (0.050 g, 0.128 mmol) and **Im-b** (0.038 g, 0.128 mmol) was transferred an 8 mL amount of benzene. The reaction mixture was stirred for 4 h at  $23$  °C. Propyne was added to the reaction mixture via gas bulb (0.128 mmol), and it was stirred for 10 h. Upon removal of solvent, the crude solid was filtered and washed with  $\text{Et}_2\text{O}$  ( $3 \times 5$  mL). Dark red **4b-Me** was isolated (0.055 g) in 69% yield.  $^1\text{H}$  NMR ( $\text{C}_6\text{D}_6$ , mult, assign):  $\delta$  6.30 (m, c), 8.23 (s, g), 4.79 (s, h), 6.96 (t, 7, j, n), 0.73 (s, r), 1.28 (d, 6, s), 2.30 (s,  $\text{CH}_3$ ).  $^{13}\text{C}\{^1\text{H}\}$  NMR ( $\text{C}_6\text{D}_6$ , mult,  $J_{\text{CF}}$  (Hz); assign):  $\delta$  133.26 (a), 157.66 (d, 260; b), 96.10 (c), 158.32 (d, 260; d), 151.54 (d, 260; e), 110.75 (f), 165.29 (g), 62.03 (h), 131.79 (i), 117.45 (j, n), 152.16 (d, 260; k, m), 139.69 (d, 260; l), 16.79 (t, 10; r), 16.06 (d, 10; s), 62.51 ( $\text{C}_a$ ), 103.34 ( $\text{C}_b$ ), 3.43 (s,  $\text{CH}_3$ ).  $^{19}\text{F}$  NMR ( $\text{C}_6\text{D}_6$ , mult,  $J_{\text{CF}}$  (Hz); assign):  $\delta$  -119.52 (dd, 22, 7; b), -161.31 (t, 21; l), -132.76 (dd, 33, 7; d), -133.99 (dd, 22, 8; k, m), -118.35 (dd, 34, 18; e).  $^{31}\text{P}\{^1\text{H}\}$  NMR ( $\text{C}_6\text{D}_6$ , mult,  $J_{\text{CF}}$  (Hz); assign):  $\delta$  16.08 (d, 62; r), 14.12 (td, 62, 11; s). Anal. Calcd for  $\text{C}_{26}\text{H}_{36}\text{F}_6\text{P}_3\text{NFe}$ : C, 49.94; H, 5.80; N, 2.24. Found: C, 50.04; H, 5.42; N, 2.45. IR:  $\nu(\text{CC})$  2081  $\text{cm}^{-1}$ .**

**6. trans-[ $\kappa\text{C,N}$ -(3,4,5-( $\text{F}_3\text{-C}_6\text{H}_2$ )/ $\text{CH}_2\text{N}$  CH(3,4,6-( $\text{F}_3\text{-C}_6\text{H}_2$ )-yl)]Fe( $\text{PMe}_3$ ) $_3$ (CCPh)] (**4b-Ph**). In a 25 mL round-bottom flask charged with  $\text{Fe}(\text{PMe}_3)_4\text{Me}_2$  (0.050 g, 0.128 mmol) and **Im-b** (0.038 g, 0.128 mmol) was transferred an 8 mL amount of benzene, and the reaction mixture was stirred for 4 h at  $23$  °C. Phenylacetylene was added to the reaction via syringe (14  $\mu\text{L}$ , 0.128 mmol), and the reaction mixture was stirred for 10 h at  $23$  °C. Upon removal of solvent, the crude solid was filtered and washed with  $\text{Et}_2\text{O}$  ( $3 \times 5$  mL). Dark red **4b-Ph** was isolated (0.070 g) in 79% yield.  $^1\text{H}$  NMR ( $\text{C}_6\text{D}_6$ , mult,  $J_{\text{CF}}$  (Hz); assign):  $\delta$  6.31 (m, c), 8.18 (s, g), 4.82 (s, h), 6.85 (t, 6; j, n), 0.74 (s, r), 1.27 (d, 5; s), 7.54 (d, 7;  $\text{C}_6\text{H}_5$ ), 7.25 (t, 7;  $\text{C}_m\text{H}$ ), 7.00 (t, 7;  $\text{C}_p\text{H}$ ).  $^{13}\text{C}\{^1\text{H}\}$  NMR ( $\text{C}_6\text{D}_6$ , mult,  $J_{\text{CF}}$  (Hz); assign):  $\delta$  133.46 (a), 160.19 (d, 260; b), 96.55 (c), 157.76 (d, 260; d), 153.53 (d, 260; e), 125.97 (f), 165.29 (g), 62.32 (h), 150.11 (i), 114.69 (j, n), 151.62 (d, 250; k, m), 149.41**

(d, 260; l), 16.65 (t, 12; r), 23.39 (d, 20; s), 120.89 (q), 121.30 (r), 130.66 (s), 129.97 ( $\text{C}_a$ ), 128.33 ( $\text{C}_m$ ), 123.35 ( $\text{C}_p$ ).  $^{19}\text{F}$  NMR ( $\text{C}_6\text{D}_6$ , mult,  $J_{\text{CF}}$  (Hz); assign):  $\delta$  -119.07 (dd, 33, 10; d), -160.97 (tt, 21, 7; l), -132.10 (dd, 33, 7; e), -133.68 (dd, 22, 8; k, m), -118.30 (dd, 20, 8; b).  $^{31}\text{P}\{^1\text{H}\}$  NMR ( $\text{C}_6\text{D}_6$ , mult,  $J_{\text{CF}}$  (Hz); assign):  $\delta$  15.68 (d, 61; r), 13.46 (td, 62, 12; s). Anal. Calcd for  $\text{C}_{31}\text{H}_{38}\text{F}_6\text{P}_3\text{NFe}$ : C, 54.17; H, 5.57; N, 2.04. Found: C, 54.36; H, 5.41; N, 2.28. IR:  $\nu(\text{CC})$  2020  $\text{cm}^{-1}$ .

**7. trans-[ $\kappa\text{C,N,C}$ -(3,4,5-( $\text{F}_3\text{-C}_6\text{H}_2$ )-yl)] $\text{CH}_2\text{N}$  CH(3,4,6-( $\text{F}_3\text{-C}_6\text{H}_2$ )-yl)]Fe( $\text{PMe}_3$ ) $_2$ ( $\text{H}_2$ ) (**5b**). **a. Observation of 5b.** Into a J. Young tube (2.1 mL volume) was added **2b** (20 mg, 0.037 mmol) in  $\text{C}_6\text{D}_6$  or toluene- $d_8$ . The tube was degassed by multiple freeze-pump-thaw cycles, and dihydrogen (660 Torr) was added at  $23$  °C. The reaction was monitored by  $^1\text{H}$  and  $^{19}\text{F}$  NMR spectroscopy.  $^1\text{H}$  NMR ( $\text{C}_6\text{D}_6$ , mult,  $J_{\text{CF}}$  (Hz); assign):  $\delta$  8.08 (s, g), 6.48 (m, c, j), 4.24 (s, h), 0.22 (t, 3; r), -13.88 (t, 12; s).  $^{19}\text{F}$  NMR ( $\text{C}_6\text{D}_6$ , mult,  $J_{\text{CF}}$  (Hz); assign):  $\delta$  -107.83 (d, 35; e), -118.85 (m, b, m), -132.15 (dd, 31, 9; d), -146.57 (dd, 20, 4; k), -166.00 (ddd, 35, 19, 7; l).  $^{31}\text{P}$  NMR ( $\text{C}_6\text{D}_6$ ):  $\delta$  20.54.**

**b.  $T_1$ (min) Measurement.** **5b** was prepared in toluene- $d_8$  and allowed to equilibrate for 48 h.  $^1\text{H}$  NMR spectra were recorded at 500 MHz, and temperature calibration was performed for each measurement ( $T$  (K),  $T_1$  (ms)): 298, 21; 288, 18; 278; 16; 268, 15; 258, 13; 238, 11; 218, 11; 198, 15. The  $T_1$ (min) value of 10.7 ms (226 K) was obtained by plotting  $\ln T_1$  (ms) vs  $1/T$  ( $\text{K}^{-1}$ ) and fitting with linear regression. The  $d(\text{H-H})$  value of 0.77 Å was calculated by assuming rapid rotation of  $\text{H}_2$  and using the following equations: dipolar relaxation,  $1/T_1 = 0.3\gamma_{\text{H}}^4(h/2\pi)^2(J(\omega) + 4J(2\omega))/r_{\text{HH}}^6$ ; spectral density function,  $J(\omega) = A\tau/(1 + \omega^2\tau^2)$ , where  $A = 0.25$  for rapid rotation. The temperature dependence of the correlation time is  $\tau = \tau_0 \exp[E_a/RT]$ , and at  $T_1$ ,  $\tau = 0.62/(2\pi\nu)$ ; simplifying,  $r_{\text{HH}} = 4.611(T_1 \text{ (min)}/\nu)^{1/6}$ .

**c.  $K_c$  Measurement.** **5b** was prepared from **2b** in  $\text{C}_6\text{D}_6$  as above and allowed to equilibrate for 48 h.  $K_c$  was calculated by direct integration of **2b**, **5b**, and  $\text{H}_2$ , and the amount of  $\text{N}_2$  in solution was estimated from the Henry's law constant of  $\text{N}_2$  in benzene and assuming the total amount of  $\text{N}_2$  (gas and solution) was equal to that of **5b**.

**8. trans-[ $\kappa\text{C,N,C}$ -(3,4,5-( $\text{F}_3\text{-C}_6\text{H}_2$ )-yl)] $\text{CH}_2\text{N}$  CH(3,4,6-( $\text{F}_3\text{-C}_6\text{H}_2$ )-yl)]Fe( $\text{PMe}_3$ ) $_2\text{NH}_3$  (**6b**). In a 100 mL bomb charged with **2b** (0.100 g) was transferred 15 mL of benzene at  $-78$  °C. An excess of ammonia dried over sodium was transferred to the bomb at  $-78$  °C. The bomb was slowly warmed to  $23$  °C, and the contents were stirred for 0.5 h. The solution turned from yellow-red to bright red and eventually bright purple. The excess ammonia and benzene were removed in vacuo. The addition of benzene and excess ammonia was repeated three times. Crude product was assayed by transferring benzene- $d_6$  to an NMR tube in the absence of  $\text{N}_2$ . Bright purple **6b** was isolated (0.096 g) in 98% yield.  $^1\text{H}$  NMR ( $\text{C}_6\text{D}_6$ , mult, assign):  $\delta$  6.44 (s, c, j), 8.14 (s, g), 3.89 (s, h), 0.37 (s, s), 0.48 (s, r).  $^{13}\text{C}\{^1\text{H}\}$  NMR ( $\text{C}_6\text{D}_6$ , mult,  $J_{\text{CF}}$  (Hz); assign):  $\delta$  150.70 (a), 161.64 (d, 240; b), 95.29 (c), 161.19 (d, 240; d), 160.65 (d, 240; e), 145.89 (f), 163.67 (g), 64.93 (h), 147.80 (i), 103.64 (j), 159.87 (d, 230; k), 149.31 (d, 230; l), 152.57 (d, 230; m), 135.51 (n), 12.51 (t, 12; r).  $^{19}\text{F}$  NMR ( $\text{C}_6\text{D}_6$ , mult,  $J_{\text{CF}}$  (Hz); assign):  $\delta$  -128.99 (d, 35; m), -168.31 (dd, 30, 20; l), -119.72 (dd, 24, 7; b), -148.39 (dd, 32, 9; e), -136.60 (dd, 20, 10; k), -135.51 (dd, 34, 7; d).  $^{31}\text{P}\{^1\text{H}\}$  NMR ( $\text{C}_6\text{D}_6$ , mult, assign):  $\delta$  21.42 (s, r). Anal. Calcd for  $\text{C}_{20}\text{H}_{26}\text{F}_6\text{N}_2\text{P}_2\text{Fe}$ : C, 45.65; H, 4.98; N, 5.32. Found: C, 45.62; H, 5.09; N, 5.35.**

**9. trans-[ $\kappa\text{C,N,C}$ -(3,4,5-( $\text{F}_3\text{-C}_6\text{H}_2$ )-yl)] $\text{CH}_2\text{N}$  CH(3,4,6-( $\text{F}_3\text{-C}_6\text{H}_2$ )-yl)]Fe( $\text{PMe}_3$ ) $_2\text{py}$  (**7b**). In a 50 mL bomb charged with  $(\text{Me}_3\text{P})_4\text{FeMe}_2$  (0.050 g, 0.128 mmol) and **Im-b** (0.039 g, 0.128 mmol) was transferred 8 mL of  $\text{Et}_2\text{O}$ , and the reaction mixture was stirred for  $>4$  h at  $23$  °C. The  $\text{Et}_2\text{O}$  and  $\text{PMe}_3$  were removed in vacuo, and the residue was triturated with  $\text{Et}_2\text{O}$  to remove excess  $\text{PMe}_3$ . Another 8 mL of  $\text{Et}_2\text{O}$  was transferred to the flask, and a solution of pyridine  $N$ -oxide in  $\text{Et}_2\text{O}$  (0.126 M) was added dropwise; this mixture was stirred for 12 h at  $60$  °C. Product **7b** was filtered and washed ( $3 \times 5$  mL) with  $\text{Et}_2\text{O}$  and crystallized at  $-78$  °C (0.053 g, 70%). The red microcrystalline solid was assayed by transferring  $\text{C}_6\text{D}_6$  to an NMR tube containing the solid, in the absence of  $\text{N}_2$ .  $^1\text{H}$  NMR ( $\text{C}_6\text{D}_6$ , mult,**

$J_{CF}$  (Hz); assign):  $\delta$  6.53 (s, c), 8.81 (s, g), 4.24 (s, h), 8.01 (s, i), 0.54 (s, r), 6.89 (d, 6; C<sub>6</sub>H), 7.10 (m, C<sub>m</sub>H, C<sub>p</sub>H). <sup>13</sup>C{<sup>1</sup>H} NMR (C<sub>6</sub>D<sub>6</sub>, mult,  $J_{CF}$  (Hz); assign):  $\delta$  135.03 (a), 161.38 (d, 250; b), 94.93 (c), 158.56 (d, 250; d), 153.06 (d, 250; e), 129.96 (f), 163.67 (g), 62.96 (h), 138.79 (i), 115.11 (j), 144.10 (d, 250; k), 134.47 (d, 250; l), 151.19 (d, 250; m), 124.47 (n), 12.03 (t, 10; r), 141.19 (C<sub>o</sub>), 124.96 (C<sub>m</sub>H), 135.27 (C<sub>p</sub>). <sup>19</sup>F NMR (C<sub>6</sub>D<sub>6</sub>, mult,  $J_{CF}$  (Hz); assign):  $\delta$  -134.48–134.77 (m, d, k, m), -119.96 (dd, 22, 7; b), -162.23 (td, 22, 4; l), -127.45 (dd, 34, 23; e). <sup>31</sup>P{<sup>1</sup>H} NMR (C<sub>6</sub>D<sub>6</sub>, mult, assign): 20.15 (s, r). Anal. Calcd for C<sub>25</sub>H<sub>28</sub>F<sub>6</sub>N<sub>2</sub>P<sub>2</sub>Fe: C, 51.04; H, 4.80; N, 4.76. Found: C, 51.02; H, 4.90; N, 4.76.

10. *trans*-{*mer*-κ-C,N,C'-(3,4,5-(F)<sub>3</sub>-C<sub>6</sub>H-2-yl)CH<sub>2</sub>N CH(3,4,6-(F)<sub>3</sub>-C<sub>6</sub>H-2-yl)Fe(PMe<sub>3</sub>)<sub>2</sub>(CNMe)} (8b). In a 50 mL round-bottom flask charged with (Me<sub>3</sub>P)<sub>4</sub>FeMe<sub>2</sub> (0.200 g, 0.512 mmol) and **Im-b** (0.155 g, 0.512 mmol) was transferred 15 mL of benzene. The reaction mixture was stirred for 4 h at 23 °C. Methyl isocyanide (27 mL, 0.512 mmol) was added to the flask with continuous stirring for 6 h at 23 °C. The solvent was removed in vacuo, and the crude solid was filtered and washed in Et<sub>2</sub>O (3 × 10 mL). Red-brown solid **8b** was isolated (0.200 g) in 69% yield. <sup>1</sup>H NMR (C<sub>6</sub>D<sub>6</sub>, mult,  $J_{CF}$  (Hz); assign):  $\delta$  6.40 (m, c, j), 8.18 (s, g), 4.32 (s, h), 0.53 (t, 4; r), 2.85 (t, 2; CH<sub>3</sub>). <sup>13</sup>C{<sup>1</sup>H} NMR (C<sub>6</sub>D<sub>6</sub>, mult,  $J_{CF}$  (Hz); assign):  $\delta$  139.19 (a), 156.94 (d, 250; b), 103.73 (c), 156.57 (d, 250; d), 150.38 (d, 250; e), 143.55 (f), 159.30 (g), 63.78 (h), 137.22 (i), 133.25 (j), 147.68 (d, 250; k), 138.53 (d, 250; l), 150.00 (d, 250; m), 157.33 (n), 14.62 (t, 12; r), 96.13 (s), 29.86 (CH<sub>3</sub>). <sup>19</sup>F NMR (C<sub>6</sub>D<sub>6</sub>, mult,  $J_{CF}$  (Hz); assign):  $\delta$  -114.16 (d, 31; m), -147.14 (ddd, 19, 10, 4; k), -119.94 (ddd, 23, 8, 2; b), -166.70 (ddd, 32, 19, 5; l), -124.57 (ddd, 33, 21, 3; e), -133.85 (ddd, 31, 10, 2; d). <sup>31</sup>P{<sup>1</sup>H} NMR (C<sub>6</sub>D<sub>6</sub>, mult, assign):  $\delta$  24.04 (s, r). Anal. Calcd for C<sub>22</sub>H<sub>26</sub>F<sub>6</sub>P<sub>2</sub>N<sub>2</sub>Fe: C, 48.02; H, 4.76; N, 5.09. Found: C, 48.09; H, 4.62; N, 5.03. IR:  $\nu$ (CN) 2073 cm<sup>-1</sup>.

11. *trans*-{*mer*-κ-C,N,C'-(3,4,5-(F)<sub>3</sub>-C<sub>6</sub>H-2-yl)CH<sub>2</sub>N CH(3,4,6-(F)<sub>3</sub>-C<sub>6</sub>H-2-yl)Fe(PMe<sub>3</sub>)<sub>2</sub>(N<sub>2</sub>CPh)} (9b). In a 10 mL round-bottom flask charged with **2b** (0.045 g, 0.084 mmol) and diphenyldiazomethane (0.017 g, 0.088 mmol) was transferred 5 mL of Et<sub>2</sub>O at -78 °C. The reaction mixture was warmed to 23 °C and stirred for 16 h. The brown solution was filtered, and solvent was removed in vacuo, leaving a dark purple microcrystalline solid (0.045 g, 0.064 mmol) in 76% yield. <sup>1</sup>H NMR (C<sub>6</sub>D<sub>6</sub>, mult,  $J_{CF}$  (Hz); assign):  $\delta$  6.37 (m, c, j), 7.78 (s, g), 3.98 (s, h), 0.34 (t, 3; r), 7.61 (d, 8; C<sub>o</sub>H), 7.30 (t, 8; C<sub>m</sub>H), 6.98 (t, 8; C<sub>p</sub>H). <sup>13</sup>C{<sup>1</sup>H} NMR (C<sub>6</sub>D<sub>6</sub>, mult, assign):  $\delta$  136.38 (a), 160.93 (b), 97.60 (c), 159.40 (d), 158.11 (e), 120.27 (f), 162.21 (g), 64.31 (h), 131.82 (i), 104.71 (j), 156.99 (k), 141.98 (l), 156.08 (m), 124.94 (n), 13.15 (r), 131.83 (p), 131.09 (q), 132.12 (C<sub>o</sub>), 126.02 (C<sub>m</sub>), 125.45 (C<sub>p</sub>). <sup>19</sup>F NMR (C<sub>6</sub>D<sub>6</sub>, mult,  $J_{CF}$  (Hz); assign):  $\delta$  -114.53 (d, 31; m), -145.55 (dd, 20, 8; k), -119.22 (dd, 22, 9; b), -132.42 (dd, 31, 9; d), -124.31 (ddd, 30, 23, 5; e), -165.49 (dd, 31, 20; l). <sup>31</sup>P NMR (C<sub>6</sub>D<sub>6</sub>, mult, assign):  $\delta$  17.52 (s, r). Anal. Calcd for C<sub>33</sub>H<sub>33</sub>F<sub>6</sub>P<sub>2</sub>N<sub>3</sub>Fe: C, 56.35; H, 4.73; N, 5.97. Found: C, 56.31; H, 4.83; N, 5.91.

12. *trans*-{*mer*-κ-C,N,C'-(3,4,5-(F)<sub>3</sub>-C<sub>6</sub>H-2-yl)CH<sub>2</sub>N CH(3,4,6-(F)<sub>3</sub>-C<sub>6</sub>H-2-yl)Fe(PMe<sub>3</sub>)<sub>2</sub>l} (11b). In a 25 mL round-bottom flask charged with **2b** (0.100 g, 0.186 mmol), [Cp<sub>2</sub>Fe]BF<sub>4</sub> (0.061 g, 0.186 mmol), and excess lithium iodide (0.075 g, 0.560 mmol) was transferred 8 mL of THF at -78 °C. The reaction mixture was warmed to 23 °C and stirred for 16 h. Solvent was removed from the olive green solution, and the crude brown solid was filtered and washed (3 × 5 mL) with toluene. The brown solid was then filtered and washed (3 × 5 mL) with pentane, leaving the green-brown paramagnetic **11b** (0.050 g, 0.079 mmol) in 42% yield. <sup>1</sup>H NMR (C<sub>6</sub>D<sub>6</sub>):  $\delta$  19.95 (2 H), 12.35 (1 H), -10.25 (1 H), -13.49 (1 H), -16.62 (18 H). Anal. Calcd for C<sub>20</sub>H<sub>23</sub>F<sub>6</sub>NP<sub>2</sub>IFe: C, 37.76; H, 3.64; N, 2.20. Found: C, 37.62; H, 3.70; N, 2.26.  $\mu_{\text{eff}}$ (296 K) = 1.9, 2.0  $\mu_{\text{B}}$ .

13. *trans*-{*mer*-κ-C,N,C'-(3,4,5-(F)<sub>3</sub>-C<sub>6</sub>H-2-yl)CH<sub>2</sub>N CH(3,4,6-(F)<sub>3</sub>-C<sub>6</sub>H-2-yl)Fe(PMe<sub>3</sub>)<sub>2</sub>l} (12b). In a 25 mL round-bottom flask charged with **2b** (0.085 g, 0.158 mmol) and triphenylmethyl chloride (0.066 g, 0.237 mmol) was transferred 8 mL of benzene at -78 °C. The reaction mixture was warmed to 23 °C and stirred for 16 h. The solvent was removed in vacuo, and the crude red solid was filtered and washed (3 × 5 mL) with hexane, leaving microcrystalline red **12b** (0.060 g, 0.110 mmol) in 70% yield. Single crystals were grown from a

concentrated solution in Et<sub>2</sub>O at -40 °C. <sup>1</sup>H NMR (C<sub>6</sub>D<sub>6</sub>):  $\delta$  12.45 (1 H), -4.61 (2 H), -9.86 (2 H), -16.52 (18 H).  $\mu_{\text{eff}}$ (296 K) = 1.9, 2.0  $\mu_{\text{B}}$ .

**Single-Crystal X-ray Diffraction Studies.** Upon isolation, the crystals were covered in polyisobutenes and placed under a 173 K N<sub>2</sub> stream on the goniometer head of a Siemens P4 SMART CCD area detector (graphite-monochromated Mo K $\alpha$  radiation,  $\lambda$  = 0.71073 Å). The structures were solved by direct methods (SHELXS). All non-hydrogen atoms were refined anisotropically unless stated, and hydrogen atoms were treated as idealized contributions (Riding model).

1. *trans*-{κ-C,N,C'-(2,4,5-tri-*uorophen*-2-yl)CH<sub>2</sub>N CH(3,4,5-tri-*uorophen*-2-yl)Fe(PMe<sub>3</sub>)<sub>2</sub> (N<sub>2</sub>)} (2b). A red block (0.25 × 0.20 × 0.15 mm) was obtained from benzene. A total of 9138 reflections were collected with 5119 determined to be symmetry independent ( $R_{\text{int}}$  = 0.0298), and 4493 were greater than  $2\sigma(I)$ . A semiempirical absorption correction from equivalents was applied, and the refinement utilized  $w^{-1} = \sigma^2(F_o^2) + (0.0437p)^2 + 0.1193p$ , where  $p = (F_o^2 + 2F_c^2)/3$ .

2. *trans*-{*mer*-κ-C,N,C'-(3,4,5-(F)<sub>3</sub>-C<sub>6</sub>H-2-yl)CH<sub>2</sub>N CH(3,4,6-(F)<sub>3</sub>-C<sub>6</sub>H-2-yl)Fe(PMe<sub>3</sub>)<sub>2</sub>Cl} (12b). A red block (0.40 × 0.15 × 0.10 mm) was obtained from diethyl ether. A total of 23077 reflections were collected with 6176 determined to be symmetry independent ( $R_{\text{int}}$  = 0.0321), and 4841 were greater than  $2\sigma(I)$ . A semiempirical absorption correction from equivalents was applied, and the refinement utilized  $w^{-1} = \sigma^2(F_o^2) + (0.0483p)^2 + 1.1000p$ , where  $p = (F_o^2 + 2F_c^2)/3$ .

**Computations.** Calculations were carried out at the M06<sup>19</sup>/6-311+G(d)<sup>20</sup> level of theory. An ultra-fine grid was used for integration in all calculations. Simulations were performed with the Gaussian 09 program.<sup>21</sup> All structures were optimized with restraint of neither symmetry nor geometry. Open-shell complexes were modeled within the framework of the unrestricted Kohn–Sham formalism; spin contamination was deemed to be minimal via calculation of the  $S^2_{\text{UDFT}}$  expectation value. Systems were judged to be minima via calculation of the energy Hessian. Quoted energetics are free energies (kcal/mol), unless specified otherwise, and were determined with unscaled vibrational frequencies assuming standard temperature and pressure.

## ASSOCIATED CONTENT

### Supporting Information

CIF files giving crystallographic data for **2b** and **12b** and text and figures giving full experimental details, including all spectral details. This material is available free of charge via the Internet at <http://pubs.acs.org>.

## AUTHOR INFORMATION

### Corresponding Author

E-mail: ptw2@cornell.edu

### Notes

The authors declare no competing financial interest.

## ACKNOWLEDGMENTS

We thank the National Science Foundation (CHE-1055505, P.T.W.), the U.S. Department of Energy (BES DE-FG02-03ER15387, T.R.C.), and Cornell University for financial support.

## REFERENCES

- (1) Howard, J. B.; Rees, D. C. *Proc. Natl. Acad. Sci. U.S.A.* **2006**, *103*, 17088–17093.
- (2) Rees, D. C.; Tezcan, F. A.; Haynes, C. A.; Walton, M. Y.; Andrade, S.; Einsle, O.; Howard, J. B. *Philos. Trans. R. Soc. A* **2005**, *363*, 971–984.
- (3) Einsle, O.; Tezcan, F. A.; Andrade, S. L. A.; Schmid, B.; Yoshida, M.; Howard, J. B.; Rees, D. C. *Science* **2002**, *297*, 1696–1700.
- (4) Hoffman, B. M.; Dean, D. R.; Seefeldt, L. C. *Acc. Chem. Res.* **2009**, *42*, 609–619.

- (5) Eady, R. R. *Chem. Rev.* **1996**, *96*, 3013–3030.
- (6) Rubio, L. M.; Ludden, P. W. *J. Bacteriol.* **2005**, *187*, 405–414.
- (7)
- (8) Hu, Y. L.; Ribbe, M. W. *Microbiol. Mol. Biol. Rev.* **2011**, *75*, 664–677.
- (9) Hu, Y. L.; Lee, C. C.; Ribbe, M. W. *Dalton Trans.* **2012**, *41*, 1118–1127.
- (10) (a) Hu, Y. L.; Ribbe, M. W. *Coord. Chem. Rev.* **2011**, *255*, 1218–1224. (b) Hu, Y. L.; Ribbe, M. W. *Acc. Chem. Res.* **2010**, *43*, 475–484.
- (11) Wiig, J. A.; Hu, Y. L.; Lee, C. C.; Ribbe, M. W. *Science* **2012**, *337*, 1672–1675.
- (12) Lancaster, K. M.; Boemelt, M.; Ettenhuber, P.; Hu, Y.; Ribbe, M. W.; Neese, F.; Bergmann, U.; DeBeer, S. *Science* **2011**, *334*, 974–976.
- (13) Spatzal, T.; Aksoyoglu, M.; Zhang, L.; Andrade, S. L. A.; Schleicher, E.; Weber, S.; Rees, D. C.; Einsle, O. *Science* **2011**, *334*, 940.
- (14) Erisman, J. W.; Sutton, M. A.; Galloway, J.; Klimont, Z.; Winiwarter, W. *Nat. Geosci.* **2008**, *1*, 636–639.
- (15) Ertl, G. *Z. Anorg. Allg. Chem.* **2012**, 487–489.
- (16) Schlogl, R. *Angew. Chem., Int. Ed.* **2003**, *42*, 2004–2008.
- (17) Ertl, G. *Angew. Chem., Int. Ed.* **2008**, *47*, 3524–3535.
- (18) Greenwood, N. N.; Earnshaw, A. *Chemistry of the Elements*, 2nd ed.; Butterworth-Heinemann (Elsevier Science): New York, 1997; Haber–Bosch, pp 421–422; Ostwald, pp 466–467. For Allen and Seno, see ref 28.
- (19) Allen, A. D.; Senoff, C. V. *Chem. Commun.* **1965**, 621–622.
- (20) Allen, A. D.; Bottomley, F.; Harris, R. O.; Reinsalu, V. P.; Senoff, C. V. *J. Am. Chem. Soc.* **1967**, *89*, 5595–5599.
- (21) (a) Leigh, G. J. *Can. J. Chem.* **2005**, *83*, 277–278. (b) Taube, H. *Coord. Chem. Rev.* **1978**, *26*, 1–5.
- (22) Chatt, J.; Dilworth, J. R.; Richards, R. L. *Chem. Rev.* **1978**, *78*, 589–625.
- (23) Richards, R. L. *Coord. Chem. Rev.* **1996**, *154*, 83–97.
- (24) Leigh, G. J. *J. Organomet. Chem.* **2004**, *689*, 3999–4005.
- (25) Leigh, G. J. *Acc. Chem. Res.* **1992**, *25*, 177–184.
- (26) Hidai, M. *Coord. Chem. Rev.* **1999**, *185*–186, 99–108.
- (27) Hidai, M.; Mizobe, Y. In *Metal Ions in Biological Systems*; Marcel Dekker: New York, 2002; Vol. 39, pp 121–161.
- (28) Weiss, C. J.; Groves, A. N.; Mock, M. T.; Dougherty, W. G.; Kassel, W. S.; Helm, M. L.; DuBois, D. L.; Bullock, R. M. *Dalton Trans.* **2012**, *41*, 4517–4529.
- (29) Bazhenova, T. A.; Shilov, A. E. *Coord. Chem. Rev.* **1995**, *144*, 69–145.
- (30) Crossland, J. L.; Tyler, D. R. *Coord. Chem. Rev.* **2010**, *254*, 1883–1894.
- (31) Hazari, N. *Chem. Soc. Rev.* **2010**, *39*, 4044–4056.
- (32) Holland, P. L. *Can. J. Chem.* **2005**, *83*, 296–301.
- (33) Ballmann, J.; Munha, R. F.; Fryzuk, M. D. *Chem. Commun.* **2010**, *46*, 1013–1025.
- (34) Gambarotta, S.; Scott, J. *Angew. Chem., Int. Ed.* **2004**, *43*, 5298–5308.
- (35) Fryzuk, M. D.; Johnson, S. A. *Coord. Chem. Rev.* **2000**, *200*–202, 379–409.
- (36) Shaver, M. P.; Fryzuk, M. D. *Adv. Synth. Catal.* **2003**, *345*, 1061–1076.
- (37) Fryzuk, M. D. *Acc. Chem. Res.* **2009**, *42*, 127–133.
- (38) Ballmann, J.; Yeo, A.; Patrick, B. O.; Fryzuk, M. D. *Angew. Chem., Int. Ed.* **2011**, *50*, 507–510.
- (39) Chirik, P. J. *Dalton Trans.* **2007**, 16–25.
- (40) Rodriguez, M. M.; Bill, E.; Brennessel, W. W.; Holland, P. L. *Science* **2011**, *334*, 780–783.
- (41) (a) Laplaza, C. E.; Johnson, M. J. A.; Peters, J. C.; Odom, A. L.; Kim, E.; Cummins, C. C.; George, G. N.; Pickering, I. J. *J. Am. Chem. Soc.* **1996**, *118*, 8623–8638. (b) Figueroa, J. S.; Piro, N. A.; Clough, C. R.; Cummins, C. C. *J. Am. Chem. Soc.* **2006**, *128*, 940–950.
- (42) Korobkov, I.; Gambarotta, S.; Yap, G. P. A. *Angew. Chem., Int. Ed.* **2002**, *41*, 3433–3436.
- (43) Nikiforov, G. B.; Vidyaratne, I.; Gambarotta, S.; Korobkov, I. *Angew. Chem., Int. Ed.* **2009**, *48*, 7415–7419.
- (44) Caselli, A.; Solari, E.; Scopelliti, R.; Floriani, C.; Re, N.; Rizzoli, C.; Chiesi-Villa, A. *J. Am. Chem. Soc.* **2000**, *122*, 3652–3670.
- (45) Kawaguchi, H.; Matsuo, T. *Angew. Chem., Int. Ed.* **2002**, *41*, 2792–2793.
- (46) Clentsmith, G. K. B.; Bates, V. M. E.; Hitchcock, P. B.; Cloke, F. G. N. *J. Am. Chem. Soc.* **1999**, *121*, 10444–10445.
- (47) Hebden, T. J.; Schrock, R. R.; Takase, M. K.; Muller, P. *Chem. Commun.* **2012**, *48*, 1851–1853.
- (48) Semproni, S. P.; Milsman, C.; Chirik, P. J. *Angew. Chem., Int. Ed.* **2012**, *51*, 5213–5216.
- (49) Pun, D.; Bradley, C. A.; Lobkovsky, E.; Keresztes, I.; Chirik, P. J. *J. Am. Chem. Soc.* **2008**, *130*, 14046–14047.
- (50) Hanna, T. E.; Keresztes, I.; Lobkovsky, E.; Chirik, P. J. *Inorg. Chem.* **2007**, *46*, 1675–1683.
- (51) (a) Bernskoetter, W. H.; Olmos, A. V.; Lobkovsky, E.; Chirik, P. J. *Organometallics* **2006**, *25*, 1021–1027. (b) Bernskoetter, W. H.; Lobkovsky, E.; Chirik, P. J. *J. Am. Chem. Soc.* **2005**, *127*, 14051–14061.
- (52) (a) Bernskoetter, W. H.; Pool, J. A.; Lobkovsky, E.; Chirik, P. J. *J. Am. Chem. Soc.* **2005**, *127*, 7901–7911. (b) Pool, J. A.; Bernskoetter, W. H.; Chirik, P. J. *J. Am. Chem. Soc.* **2004**, *126*, 14326–14327. (c) Pool, J. A.; Lobkovsky, E.; Chirik, P. J. *Nature* **2004**, *427*, 527–530.
- (53) Yandulov, D. V.; Schrock, R. R. *Science* **2003**, *301*, 76–78.
- (54) (a) Schrock, R. R. *Acc. Chem. Res.* **2005**, *38*, 955–962. (b) Schrock, R. R. *Angew. Chem., Int. Ed.* **2008**, *47*, 5512–5522.
- (55) Nishibayashi, Y. *Dalton Trans.* **2012**, *41*, 7447–7453.
- (56) Arashiba, K.; Miyake, Y.; Nishibayashi, Y. *Nat. Chem.* **2011**, *3*, 120–125.
- (57) Tanaka, H.; Sasada, A.; Kouno, T.; Yuki, M.; Miyake, Y.; Nakanishi, H.; Nishibayashi, Y.; Yoshizawa, K. *J. Am. Chem. Soc.* **2011**, *41*, 3498.
- (58) (a) Knobloch, D. J.; Semproni, S. P.; Lobkovsky, E.; Chirik, P. J. *J. Am. Chem. Soc.* **2012**, *134*, 3377–3386. (b) Semproni, S. P.; Lobkovsky, E.; Chirik, P. J. *J. Am. Chem. Soc.* **2011**, *133*, 10406–10409. (c) Knobloch, D. J.; Lobkovsky, E.; Chirik, P. J. *J. Am. Chem. Soc.* **2010**, *132*, 15340–15350. (d) Knobloch, D. J.; Lobkovsky, E.; Chirik, P. J. *J. Am. Chem. Soc.* **2010**, *132*, 10553–10564. (e) Knobloch, D. J.; Lobkovsky, E.; Chirik, P. J. *Nat. Chem.* **2010**, *2*, 30–35.
- (59) Bernskoetter, W. H.; Lobkovsky, E.; Chirik, P. J. *Angew. Chem., Int. Ed.* **2007**, *46*, 2858–2861.
- (60) Mori, M.; Hori, K.; Akashi, M.; Hori, M.; Sato, Y.; Nishida, M. *Angew. Chem., Int. Ed.* **1998**, *37*, 636–637.
- (61) (a) Manriquez, J. M.; Bercaw, J. E. *J. Am. Chem. Soc.* **1974**, *96*, 6229–6230. (b) Manriquez, J. M.; Sanner, R. D.; Marsh, R. E.; Bercaw, J. E. *J. Am. Chem. Soc.* **1976**, *98*, 3042–3044.
- (62) Smith, J. M.; Sadique, A. R.; Cundari, T. R.; Rodgers, K. R.; Lukat-Rodgers, G.; Lachicotte, R. J.; Flaschenriem, C. J.; Vela, J.; Holland, P. L. *J. Am. Chem. Soc.* **2006**, *128*, 756–769.
- (63) Smith, J. M.; Subedi, D. *Dalton Trans.* **2012**, *41*, 1423–1429.
- (64) Saouma, C. T.; Peters, J. C. *Coord. Chem. Rev.* **2011**, *255*, 920–937.
- (65) Hohenberger, J.; Ray, K.; Meyer, K. *Nat. Commun.* **2012**, *3*, 1–13.
- (66) (a) Betley, T. A.; Peters, J. C. *J. Am. Chem. Soc.* **2004**, *126*, 6252–6254. (b) Rohde, J.-U.; Betley, T. A.; Jackson, T. A.; Saouma, C. T.; Peters, J. C.; Que, L. *Inorg. Chem.* **2007**, *46*, 5720–5726.
- (67) Vogel, C.; Heinemann, F. W.; Sutter, J.; Anthon, C.; Meyer, K. *Angew. Chem., Int. Ed.* **2008**, *47*, 2681–2684.
- (68) Scepaniak, J. J.; Young, J. A.; Bontchev, R. P.; Smith, J. M. *Angew. Chem., Int. Ed.* **2009**, *48*, 3158–3160.
- (69) Scepaniak, J. J.; Bontchev, R. P.; Johnson, D. L.; Smith, J. M. *Angew. Chem., Int. Ed.* **2011**, *50*, 6630–6633.
- (70) Scepaniak, J. J.; Vogel, C. S.; Khusniyarov, M. M.; Heinemann, F. W.; Meyer, K.; Smith, J. M. *Science* **2011**, *331*, 1049–1052.
- (71) Berry, J. F.; Bill, E.; Bothe, E.; George, S. D.; Bienert, B.; Neese, F.; Wiegardt, K. *Science* **2006**, *312*, 1937–1941.
- (72) Aliaga-Alcalde, N.; George, S. D.; Mienert, B.; Bill, E.; Wiegardt, K.; Neese, F. *Angew. Chem., Int. Ed.* **2005**, *44*, 2908–2912.

- (73) Meyer, K.; Bill, E.; Mienert, B.; Weyhermueller, T.; Wieghardt, K. *J. Am. Chem. Soc.* **1999**, *121*, 4859–4876.
- (74) Wagner, W. D.; Nakamoto, K. *J. Am. Chem. Soc.* **1989**, *111*, 1590–1598.
- (75) Walstrom, A.; Pink, M.; Yang, X.; Tomaszewski, J.; Baik, M.-H.; Caulton, K. G. *J. Am. Chem. Soc.* **2005**, *127*, 5330–5331.
- (76) Askevold, B.; Nieto, J. T.; Tussupbayev, S.; Diefenbach, M.; Herdtweck, E.; Holthausen, M. C.; Schneider, S. *Nat. Chem.* **2011**, *3*, 532–537.
- (77) (a) Moret, M.-E.; Peters, J. C. *J. Am. Chem. Soc.* **2011**, *133*, 18118–18121. (b) Moret, M.-E.; Peters, J. C. *Angew. Chem., Int. Ed.* **2011**, *50*, 2063–2067.
- (78) Saouma, C. T.; Moore, C. E.; Rheingold, A. L.; Peters, J. C. *Inorg. Chem.* **2011**, *50*, 11285–11287.
- (79) Takaoka, A.; Mankad, N. P.; Peters, J. C. *J. Am. Chem. Soc.* **2011**, *133*, 8440–8443.
- (80) Lee, Y.; Mankad, N. P.; Peters, J. C. *Nat. Chem.* **2010**, *2*, 558–565.
- (81) Whited, M. T.; Mankad, N. P.; Lee, Y. H.; Oblad, P. F.; Peters, J. C. *Inorg. Chem.* **2009**, *48*, 2507–2517.
- (82) Hendrich, M. P.; Gunderson, W.; Behan, R. K.; Green, M. T.; Mehn, M. P.; Betley, T. A.; Lu, C. C.; Peters, J. C. *Proc. Natl. Acad. Sci. U.S.A.* **2006**, *103*, 17107–17112.
- (83) Gilbertson, J. D.; Szymczak, N. K.; Tyler, D. R. *J. Am. Chem. Soc.* **2005**, *127*, 10184–10185.
- (84) (a) Crossland, J. L.; Balesdent, C. G.; Tyler, D. R. *Inorg. Chem.* **2012**, *51*, 439–445. (b) Crossland, J. L.; Young, D. M.; Zakharov, L. N.; Tyler, D. R. *Dalton Trans.* **2009**, 9253–9259. (c) Crossland, J. L.; Balesdent, C. G.; Tyler, D. R. *Dalton Trans.* **2009**, 4420–4422. (d) Crossland, J. L.; Zakharov, L. N.; Tyler, D. R. *Inorg. Chem.* **2007**, *46*, 10476–10478. (e) Gilbertson, J. D.; Szymczak, N. K.; Crossland, J. L.; Miller, W. K.; Lyon, D. K.; Foxman, B. M.; Davis, J.; Tyler, D. R. *Inorg. Chem.* **2007**, *46*, 1205–1214.
- (85) (a) Sellmann, D.; Hille, A.; Rosler, A.; Heinemann, F. W.; Moll, M.; Brehm, G.; Schneider, S.; Reiher, M.; Hess, B. A.; Bauer, W. *Chem. Eur. J.* **2004**, *10*, 820–830. (b) Sellmann, D.; Hille, A.; Heinemann, F. W.; Moll, M.; Reiher, M.; Hess, B. A.; Bauer, W. *Chem. Eur. J.* **2004**, *10*, 4214–4224.
- (86) Saouma, C. T.; Muller, P.; Peters, J. C. *J. Am. Chem. Soc.* **2009**, *131*, 10358–10359.
- (87) Saouma, C. T.; Kinnery, R. A.; Hoffman, B. M.; Peters, J. C. *Angew. Chem., Int. Ed.* **2011**, *50*, 3446–3449.
- (88) Yuki, M.; Miyake, Y.; Nishibayashi, Y. *Organometallics* **2012**, *31*, 2953–2956.
- (89) Haring, H. W., Ed. *Industrial Gases Processing*; Wiley-VCH: Weinheim, Germany, 2008.
- (90) Kerry, F. G. *Industrial Gas Handbook: Gas Separation and Purification*; CRC Press, Taylor and Francis Group: Boca Raton, FL, 2007.
- (91) Kidnay, A. J.; Parrish, W. R.; McCartney, D. G. *Fundamentals of Natural Gas Processing*, 2nd ed.; CRC Press, Taylor and Francis Group: Boca Raton, FL, 2011.
- (92) Allen, A. D.; Bottomley, F. *Can. J. Chem.* **1968**, *46*, 469.
- (93) Aresta, M.; Giannoccaro, P.; Rossi, M.; Sacco, A. *Inorg. Chim. Acta* **1971**, *5*, 203–206.
- (94) Giannoccaro, P.; Rossi, M.; Sacco, A. *Coord. Chem. Rev.* **1972**, *8*, 77–79.
- (95) Franke, O.; Wiesler, B. E.; Lehnert, N.; Nather, C.; Ksenofontov, V.; Neuhausen, J.; Tuzcek, F. *Inorg. Chem.* **2002**, *41*, 3491–3499.
- (96) (a) Franke, O.; Wiesler, B. E.; Lehnert, N.; Peters, G.; Burger, P.; Tuzcek, F. *Z. Anorg. Allg. Chem.* **2006**, *632*, 1247–1256. (b) Studt, F.; Tuzcek, F. *J. Comput. Chem.* **2006**, *27*, 1278–1291.
- (97) de la Jara Leal, A.; Tenorio, M. J.; Puerta, M. C.; Valerga, P. *Organometallics* **1995**, *14*, 3839–3847.
- (98) Volpe, E. C.; Wolczanski, P. T.; Lobkovsky, E. B. *Organometallics* **2010**, *29*, 364–377.
- (99) Karsch, H. H. *Chem. Ber.* **1977**, *110*, 2699–2711.
- (100) (a) Camadanli, S.; Beck, R.; Florke, U.; Klein, H. F. *Organometallics* **2009**, *28*, 2300–2310. (b) Beck, R.; Zheng, T.; Sun, H.; Li, X.; Florke, U.; Klein, H.-F. *J. Organomet. Chem.* **2008**, *693*, 3471–3478. (c) Beck, R.; Sun, H.; Li, X.; Camadanli, S.; Klein, H.-F. *Eur. J. Inorg. Chem.* **2008**, 3253–3257. (d) Klein, H.-F.; Camadanli, S.; Beck, R.; Leukel, D.; Florke, U. *Angew. Chem., Int. Ed.* **2005**, *44*, 975–977. (e) Klein, H.-F.; Camadanli, S.; Beck, R.; Florke, U. *Chem. Commun.* **2005**, 381–382.
- (101) (a) Liu, N.; Li, X.; Sun, H. *J. Organomet. Chem.* **2011**, *696*, 2537–2542. (b) Shi, Y.; Li, M.; Hu, Q.; Li, X.; Sun, H. *Organometallics* **2009**, *28*, 2206–2210.
- (102) Bhattacharya, P.; Krause, J. A.; Guan, H. R. *Organometallics* **2011**, *30*, 4720–4729.
- (103) (a) Martin, A. *Chem. Rev.* **2010**, *110*, 576–623. (b) Kulkarni, A. A.; Daugulis, O. *Synthesis* **2009**, 4087–4109.
- (104) (a) Evans, D. F. *J. Chem. Soc.* **1959**, 2003–2005. (b) Schubert, E. M. *J. Chem. Educ.* **1992**, *69*, 62.
- (105) (a) Figgis, B. N.; Hitchman, M. A. *Ligand Field Theory and Its Applications*; Wiley-VCH: New York, 2000. (b) Carlin, R. L. *Magnetochemistry*; Springer-Verlag: New York, 1986.
- (106) Zhang, G.; Musgrave, C. B. *J. Phys. Chem. A* **2007**, *111*, 1554–1561.
- (107) (a) Poli, R.; Cacelli, I. *Eur. J. Inorg. Chem.* **2005**, *12*, 2324–2331. (b) Petit, A.; Cacelli, I.; Poli, R. *Chem. Eur. J.* **2006**, *12*, 813–823.
- (108) (a) Sydora, O. L.; Wolczanski, P. T.; Lobkovsky, E. B.; Buda, C.; Cundari, T. R. *Inorg. Chem.* **2005**, *44*, 2606–2618. (b) Kuiper, D. S.; Douthwaite, R. E.; Mayol, A.-R.; Wolczanski, P. T.; Lobkovsky, E. B.; Cundari, T. R.; Lam, O. P.; Meyer, K. *Inorg. Chem.* **2008**, *47*, 7139–7153. (c) Kuiper, D. S.; Wolczanski, P. T.; Lobkovsky, E. B.; Cundari, T. R. *J. Am. Chem. Soc.* **2008**, *130*, 12931–12943. (d) Kuiper, D. S.; Wolczanski, P. T.; Lobkovsky, E. B.; Cundari, T. R. *Inorg. Chem.* **2008**, *47*, 10542–10553.
- (109) Field, L. D.; Hazari, N.; Li, H. L.; Luck, I. J. *Magn. Reson. Chem.* **2003**, *41*, 709–713.
- (110) (a) Chang, C. J.; Harman, W. H. *J. Am. Chem. Soc.* **2007**, *129*, 15128–15129. (b) Piro, N. A.; Lichterman, M. F.; Harman, W. H.; Chang, C. J. *J. Am. Chem. Soc.* **2011**, *133*, 2108–2111.
- (111) (a) Brown, S. D.; Betley, T. A.; Peters, J. C. *J. Am. Chem. Soc.* **2003**, *125*, 322–323. (b) Brown, S. D.; Peters, J. C. *J. Am. Chem. Soc.* **2005**, *127*, 1913–1923. (c) Thomas, C. M.; Mankad, N. P.; Peters, J. C. *J. Am. Chem. Soc.* **2006**, *128*, 4956–4957.
- (112) Cowley, R. E.; Eckert, N. A.; Elhaik, J.; Holland, P. L. *Chem. Commun.* **2009**, 1760–1762.
- (113) Kubas, G. J. *Metal-Dihydrogen and Sigma-Bond Complexes: Structure, Theory, and Reactivity*; Kluwer Academic: New York, 2001.
- (114) (a) Heinekey, D. M.; Oldham, W. J., Jr. *Chem. Rev.* **1993**, *93*, 913–926. (b) Jessop, P. G.; Morris, R. H. *Coord. Chem. Rev.* **1992**, *121*, 155–284. (c) Crabtree, R. H. *Angew. Chem., Int. Ed. Engl.* **1993**, *32*, 789–805.
- (115) Szymczak, N. K.; Tyler, D. R. *Coord. Chem. Rev.* **2008**, *252*, 212–230.
- (116) (a) Bautista, M. T.; Earl, K. A.; Maltby, P. A.; Morris, R. H. *J. Am. Chem. Soc.* **1988**, *110*, 7031–7036. (b) Earl, K. A.; Jia, G.; Maltby, P. A.; Morris, R. H. *J. Am. Chem. Soc.* **1991**, *113*, 3027–3039.
- (117) Desrosiers, P. J.; Cai, L.; Lin, Z.; Richards, R.; Halpern, J. *J. Am. Chem. Soc.* **1991**, *113*, 4173–4184.
- (118) Sydora, O. L.; Kuiper, D. S.; Wolczanski, P. T.; Lobkovsky, E. B.; Dinescu, A.; Cundari, T. R. *Inorg. Chem.* **2006**, *45*, 2008–2021.
- (119) Zhao, Y.; Truhlar, D. G. *Acc. Chem. Res.* **2008**, *41*, 157–167.
- (120) Krishnan, R.; Binkley, J. S.; Seeger, R.; Pople, J. A. *J. Chem. Phys.* **1980**, *72*, 650–654.
- (121) Frisch, M. J.; Trucks, G. W.; Schlegel, H. B.; Scuseria, G. E.; Robb, M. A.; Cheeseman, J. R.; Scalmani, G.; Barone, V.; Mennucci, B.; Petersson, G. A.; Nakatsuji, H.; Caricato, M.; Li, X.; Hratchian, H. P.; Izmaylov, A. F.; Bloino, J.; Zheng, G.; Sonnenberg, J. L.; Hada, M.; Ehara, M.; Toyota, K.; Fukuda, R.; Hasegawa, J.; Ishida, M.; Nakajima, T.; Honda, Y.; Kitao, O.; Nakai, H.; Vreven, T.; Montgomery, J. A., Jr.; Peralta, J. E.; Ogliaro, F.; Bearpark, M.; Heyd, J. J.; Brothers, E.; Kudin,



K. N.; Staroverov, V. N.; Kobayashi, R.; Normand, J.; Raghavachari, K.; Rendell, A.; Burant, J. C.; Iyengar, S. S.; Tomasi, J.; Cossi, M.; Rega, N.; Millam, J. M.; Klene, M.; Knox, J. E.; Cross, J. B.; Bakken, V.; Adamo, C.; Jaramillo, J.; Gomperts, R.; Stratmann, R. E.; Yazyev, O.; Austin, A. J.; Cammi, R.; Pomelli, C.; Ochterski, J. W.; Martin, R. L.; Morokuma, K.; Zakrzewski, V. G.; Voth, G. A.; Salvador, P.; Dannenberg, J. J.; Dapprich, S.; Daniels, A. D.; Farkas, O.; Foresman, J. B.; Ortiz, J. V.; Cioslowski, J.; Fox, D. J. *Gaussian 09, Revision A.1*; Gaussian, Inc., Wallingford, CT, 2009.

(122) Harris, T. V.; Szilagy, R. K. *Inorg. Chem.* **2011**, *50*, 4811–4824.